RESERVOIR AND PRODUCTION ENGINEERING OF WELL A-18 IN THE LOS AZUFRES GEOTHERMAL FIELD IN MEXICO

Pedro Sánchez Upton+
UNU Geothermal Training Programme
National Energy Authority
Grensásvegur 9
108 Reykjavík
Iceland

+Permanent address:
Comisión Federal de Electricidad
Gerencia de Proyectos Geotermoeléctricos
Depto. de Evaluación de Pozos y Yacimientos Geotérmicos
Morelia, Michoacán
México

ABSTRACT

Reservoir and production engineering tools are applied to data obtained in a pressure buildup test on well A-18 in the Los Azufres geothermal field in México. The well produces a two-phase mixture through a single fracture in a double-porosity media. The reservoir parameters were estimated as follows: permeability-thickness between 5.4 to 8.1 X 10^{-12} m^3 (18,000 to 27,000 md-ft); the ratio of fissure system storativity to that of the total fissure-matrix system 0.1.
Test interpretation showed the presence of a sealing boundary near the well. Using estimated reservoir parameters the simulation of an idealized well producing at constant mass flow rate near a linear boundary was done considering both homogeneous and double-porosity reservoirs.

TABLE OF CONTENTS

LIST OF TABLES

LIST OF FIGURES

1. INTRODUCTION

At Well A-18 in the Los Azufres Geothermal Field, there will be installed a 5 MW_e non-condensing turbo-generator unit, to be commissioned in 1987, according to México's National Geothermoelectric Expansion Program.

In order to know the initial characteristic of this well before starting its exploitation, several tests have been carried out: pressure transient tests, and production tests.

The importance of these and other tests is because their interpretation can be used to predict the well's behaviour and also permits the taking of quick decisions to repair a well or drill another one.

The above mentioned is applied directly to a specific well, however, the reservoir parameters obtained from the tests must be utilized in the total reservoir model to predict the complete system behaviour and also to decide between different alternatives.

In the present work, practical tools to estimate reservoir parameters from a pressure buildup test are presented.

2. LOS AZUFRES FIELD

Geothermal prospecting studies in México started at the beginning of the 1950s Alonso (1985). At the present, there are more than 60 known areas which discharge geothermal fluids on the surface. On Figure 1 are presented some of these, taking into account their importance.

The Pathé zone in the state of Hidalgo was the first geothermal area where wells were drilled to generate electricity. This was done because of the relatively short distance to México City, where the consumption of electrical energy has always been high. The mass flow rate was poor and the heat content (specific enthalpy) low. However, there was installed the first geothermoelectric plant, generating about 600 kW_e. The importance of Pathé is because it was demonstrated to be feasible to exploit the geothermal resource to generate electricity.

The four most important fields in México are: Cerro Prieto, Los Azufres, Los Humeros and La Primavera. Razo (1985) presents the geological, geophysical and geochemical characteristics of these and other zones. Molinar (1985) shows a general view about the evaluation of these fields.

Well A-18, was drilled in the Los Azufres geothermal field, which is located in the state of Michoacán (Reyes, 1985), 200 km north-west from México City. The reservoir is classified as liquid-dominated and has a surface area of about 30 km^2. More than 50 wells have been drilled (Figure 2). Although the studies indicate the existence of one reservoir, the field has been divided into two parts; namely, north and south zones. In the north zone, most of the producing wells discharge a two-phase mixture. On the other hand, in the south zone there are about 4 wells which produce superheated steam. The specific enthalpy ranges from 1000 to 2850 kJ/kg, and the best steam well produces about 30 kg/s.

The reservoir has been commercially exploited since 1982, using

5 non-condensing turbo-generator units (Ortega, 1985). The nominal capacity of each unit is 5 MW_e and the admission steam pressure and mass flow rate are 0.8 MPa and 16.4 kg/s, respectively. The separated water is injected into the subsurface to avoid ecological deterioration.

Alonso (1985) has presented the expected National Geothermoelectric Expansion Program. For the case of Los Azufres the installation of some 7 small-scale turbo-generator units is planned, similar to those already installed, and also the installation of the large-scale Tejamaniles Geothermoelectric Central in the south zone. The nominal capacity of the central is 50 MW_e. According to this program, and considering the flow characteristics of all the wells, it was decided to use the well A-18 to supply one of this small units.

3. WELL CHARACTERISTICS

3.1. Well Completion

Well A-18 was drilled in the south zone of the Los Azufres field, close to an area where most of the wells produce superheated steam at relatively shallow depths (about 700 m). It was completed at 1328 m depth using the following pipes: 13-3/8" from 0 to 300 m; 9-5/8" from 0 to 1000 m; 7" from 959 to 1328 m. In Figure 3 is presented the completion of this well, the beginning of the slotted can be easily distinguished at 1013 m depth. Completions like this are common at Los Azufres.

3.2. Output Curve

In March 1986 the output characteristic curve of this well was obtained. The maximum total mass flow rate was calculated to be as high as 43 kg/s; the specific enthalpy of the mixture as 1764 kJ/kg; while the wellhead pressure was measured 0.9 MPa (Table 1). In Figure 4 are presented the steam and water characteristic curves, both at atmospheric conditions. In Table 1 the specific enthalpy of the mixture increases as the mass flow rate increases too. This effect occurs when there is a heat transfer process from the rock matrix to the fluid. In Table 1 and Figure 4 is possible to appreciate that the production of the well is controlled by the reservoir.

4. PRESSURE BUILDUP MEASUREMENTS

4.1. Test Description

On March 17, 1986, well A-18 was opened to carry out a pressure buildup test. According to field experiences acquired for several years in this matter, the well was left to produce for two days in order to reach a stable production state before the test was commenced. The flow rate was controlled by using a 2 inch orifice, installed close to the wellhead in the pipeline to the silencer. Since the production started, the common surface measurements were periodically taken and registered. Few hours before the test started, pressure and temperature logs were run to know the state of the fluid flowing into the well. After that, the test was developed using both temperature and pressure recorders.

4.2. Measurements Before Shut-In

During the drawdown period (production), three basic parameters were registered at the surface: the wellhead pressure P_{wh}, critical lip pressure P_c and head of water in weir box. The measured quantities were

$$P_{wh} = 3.2 \text{ MPa}$$
$$P_c = 0.077 \text{ MPa}$$
$$A = 0.138 \text{ m}$$

The diameter of the discharge pipe was 0.1985 m.

Simultaneous pressure and temperature logs were run downhole. The measured pressure and temperature values are reported in Table 2 and their plots against depth are shown in Figures 5 and 6, respectively. These data were also used to construct Figures 7 and 8 which will be discussed later.

4.3. Measurements During Buildup

Before the well was shut-in, pressure and temperature elements were lowered to 1200 m depth. Kuster elements recorded the pressure and temperature behaviour during a 19 hours test period. After that, the elements were brought to the surface, and the registered deflections on the metallic charts were read. The information obtained in this test is presented in Table 3. Pressure and temperature data were also plotted against the elapsed time and they are shown in Figures 9 and 10.

5. FLOWING CONDITIONS

5.1. Specific Enthalpy and Mass Flow Rate

To estimate the mass flow rate and the specific enthalpy of the fluid during the discharging period (drawdown), the empirical relation of James (1962) was employed. That expression is written in S.I. units as

$$w = \mathrm{Exp}(16.394)\ D_d^{2}\ P_c^{0.96}\ h_o^{-1.102} \qquad (1)$$

For the case of Los Azufres, where the atmospheric pressure is 0.073 MPa, one has from steam tables (Keenan et al., 1978) the following

$$v_l = 1.0368\ \text{E-03}\ m^3/kg$$
$$h_{ls} = 2280.48\ kJ/kg$$
$$h_s = 2661.8\ kJ/kg$$

where, v_l is the specific volume of liquid water, h_{ls} is the latent heat content, and h_s the steam heat content. To determine the liquid water flow rate through a V-notch (90°) weir box (ASME, 1971), one can use

$$w_l = 1.3345\ A^{2.475}/v_l \qquad (2)$$

where A is the head of water in m, and w_l the water flow rate in kg/s. Substituting v_l into Equation 2, one gets

$$w_l = 1287.16\ A^{2.475} \qquad (3)$$

The steam fraction is defined at atmospheric conditions as

$$X = w_s/(w_l + w_s) = (h_o - h_l)/h_{ls} \qquad (4)$$

where, w_s is the steam flow rate in kg/s, h_o is the specific enthalpy of the steam-water mixture in kJ/kg (assuming that the stagnation and the steam-water mixture enthalpies are equal),

and h_l the liquid water heat content in kJ/kg. From Equation 4 one has

$$w = w_l h_{l\,s}/(h_s - h_o) \qquad (5)$$

Substituting Equation 3 into Equation 5 with the values of the enthalpies for Los Azufres one gets

$$w = \mathrm{Exp}(14.8923)\ A^{2.475}/(2661.8 - h_o) \qquad (6)$$

The final expression in terms of the stagnation enthalpy is derived from Equation 1 and 6, and can be written as

$$F(h_o) = a_1\ D_d^2\ P_c^{0.96}\ h_o^{-1.102}\ (2661.8 - h_o) - A^{2.475} = 0 \qquad (7)$$

where

$$a_1 = 4.487$$

The latter equation must be solved for h_o using a mathematical convergence method (e.g. Newton-Raphson). After that process, one has to come back to the expression which contains the mass flow rate. The computed values for both; the specific stagnation enthalpy; and the mass flow rate were found, respectively

$$h_o = 1314 \quad \mathrm{kJ/kg}$$
$$w = 16.2 \quad \mathrm{kg/s}$$

The lip pressure was not corrected for the presence of gas in the mixture because the amount of gas present was not available but is it generally low in Los Azufres.

5.2. Pressure and Temperature Logs

Returning to the flowing pressure profile in Figure 5, it is possible to distinguish three different straight lines. The first straight line starts at the surface and finishes where the intersection with the second line occurs at 950 m depth. The change in slope between the first and the second straight

lines is due to the reduction in pipe diameter. The intersection of the second and third straight lines is located at 1225 m depth. Here the change in slope is related to the feed zone. Flowing temperature profile (Figure 6) shows an almost typical temperature distribution inside a geothermal well. However at about 1250 m depth there is a small temperature inversion which also can be related to the feed zone.

5.3. Fluid Thermodynamic State

In order to know the state of the fluid throughout the well during flowing, the Clapeyron Diagram in Figure 7 was utilized. Pressure and temperature data under flowing conditions were plotted on the diagram. It was possible to determine that two-phase flow occurs between from approximately 1225 m depth and to the surface. The presence of a single liquid water phase was detected below that depth.

5.4. Wellbore Simulation

Taking into account the calculated specific enthalpy and mass flow rate as well as the measured wellhead pressure and the well completion, a program used by Ambastha and Gudmundsson (1986), was run from top to bottom. The data and output are presented in Appendix A. The measured and calculated pressures can be observed and compared in Figure 8. This plot shows that the simulator gave reasonable fit. Although not presented, the temperature profile was also a good fit.

5.5. Feed Zone Depth

After analyzing the information available and employing the results of the simulator the feed zone was determined to be between 1200 and 1250 m depth. Below that depth, the pressure increases according to a hydraulic column, that can be due to a small or non-production horizon.

6. INTERPRETATION OF BUILDUP TEST

6.1. Pressure and Temperature Buildup

In the Clapeyron Diagram (Figure 11) is presented the thermodynamic behaviour of the fluid at 1200 m depth during the buildup test. The thermodynamic state of the fluid was in the compressed liquid region.

6.2. Identification of Model

6.2.1. Inner boundary

Pressure transient test interpretation starts by plotting the pressure increment δP against the time increment δt a log-log paper as shown in Figure 12. The inner boundary effect is felt at the earlier elapsed time (Gringarten, 1985). The dominant effect can be: wellbore storage, skin, fracture, and partial penetration.

Wellbore storage effect is due to expansion of the fluid inside the well and is characterized by a straight line of one unit slope in the diagnostic plot (Figure 12). Skin effect is due to the presence of some damage in the walls of the well and it produces a steady state pressure drop. Partial penetration results from uncompleted drilling process through the total reservoir thickness (normally found in geothermics). Fractures exhibit on a log-log plot a straight line with one-half slope when it has a very high conductivity or one-quarter slope when the conductivity is low.

The inner boundary was determined to be a single medium conductivity fracture because the slope of the fitted straight line which passes through the earliest points (Figure 12) is between the one-half and one-quarter slopes.

6.2.2. Reservoir behaviour

Gringarten (1985) defines reservoirs according to their response, as homogeneous or heterogeneous. These responses can be very similar when the data are not properly plotted on log-log paper (scale problem). However, it is possible to avoid that confusion by plotting the derivative $d(\delta P)/d(Ln(\delta t))$ against δt on the same kind of paper.

This idea was considered to apply directly to the test data, however, there was noise in the results and that made it difficult to distinguish clearly the reservoir response. Least squares method was used to smooth the data. In Figure 13 is presented δP against $Ln(\delta t)$ on Cartesian axis for both cases: measured and fitted data. The fitted curve is

$$\delta P = A_1 + A_2 * Z + A_3 * Z^2 + A_4 * Z^3 + A_5 * Z^4 \qquad (8)$$

where

$A_1 = 3.634032$
$A_2 = -2.113564$
$A_3 = 0.4576055$
$A_4 = -4.222444E-02$
$A_5 = 1.415709E-03$
$Z = Ln(\delta t)$

with

Coefficient of determination = 0.995
Coefficient of correlation = 0.998
Standard error of estimate = 2.79D-03

Therefore the fit was reasonable, and derivative function becomes

$$d(\delta P)/d(Ln(\delta t)) = A_2 + 2*A_3*Z + 3*A_4*Z^2 + 4*A_5*Z^3 \qquad (9)$$

Plotting the derivative function as described before, Figure 14 was obtained, which shows the characteristic hump of a heterogeneous reservoir response (Gringarten 1985). Now going back to Figure 12, one can appreciate in the infinite acting

period two straight lines with the same slope, which is typical of double-porosity reservoirs.

6.2.3. Outer boundary

At late time, it is possible to observe a faster pressure increment in the diagnostic plot (Figure 12), which is the characteristic of an outer boundary. To determine the type of boundary, it was necessary to construct the specialized plot shown in Figure 15. One can see that the slope of the late time straight line is twice the total system reservoir slope. This is due to the existence of a sealing fault near the well.

6.2.4. Complete reservoir behaviour

The complete behaviour is obtained by combining the individual behaviors. In that way, the complete behaviour is defined as: a single medium conductivity fracture in a double-porosity reservoir with a sealing fault boundary.

6.3. Available Theory and Solutions

6.3.1. Homogeneous reservoir

Based on Earlougher (1977) the classical equation which describes isothermal radial flow of a fluid throughout a homogeneous and isotropic medium, can be written as

$$\delta^2 P/\delta r^2 + 1/r \;\; \delta P/\delta r = (\phi C_t \mu/k) \; \delta P/\delta t \qquad (10)$$

This expression is called the diffusivity equation, it assumes Darcian flow of a fluid of slight compressibility, through a medium of constant thickness, due the presence of a small pressure gradients. The term $(k/\phi C_t \mu)$ is called hydraulic diffusivity. Solution of the diffusivity equation for the case of constant flow rate production in an infinite reservoir can be written as

$$P_i - P(r,t) = (q\mu/4\pi kH)\ [-Ei\ (-\phi C_t \mu r^2/4kt)\ ] \qquad (11)$$

where Ei is the exponential integral. When the exponential integral argument is lower than 0.01, it can be approximated by

$$-Ei\ [-(\phi C_t \mu r^2/4kt)] \approx Ln\ [4kt/Exp(\Gamma)\phi C_t \mu r^2] \qquad (12)$$

Substituting Equation 12 into Equation 10 and remembering that q= wv, gives

$$P_i - P(r,t) = (wv\mu/4\pi kH)\ Ln[4kt/Exp(\Gamma)\phi C_t \mu r^2] \qquad (13)$$

for the case of a well ($r=r_w$) which produces from all the reservoir thickness, and considering the skin factor

$$P_{wf} = P_i - (wv\mu/4\pi kH)\ [\ Ln\ (4kt/Exp(\Gamma)\phi C_t \mu r_w^2) + 2s] \qquad (14)$$

Defining dimensionless time as

$$t_D = kt/\phi C_t \mu r_w^2 \qquad (15)$$

the dimensionless radius by

$$r_D = r/r_w \qquad (16)$$

and the dimensionless pressure as

$$P(r_D, t_D) = (2\pi kH/wv\mu)\ [P_i - P(r,t)] \qquad (17)$$

For the dimensionless case, in which the mechanical skin factor is considered, one has from Equation 17 the following

$$P(1,t_D) + s = P(t_D) + s = (2\pi kH/wv\mu)\ [P_i - P_{wf}] \qquad (18)$$

Substituting Equation 18 into Equation 14 and canceling similar terms

$$P(t_D) = 0.5 \text{ Ln } [4kt/\text{Exp}(\Gamma)\phi C_t \mu r_w^2] \quad (19)$$

Equation 19 can be re-written using Equations 15 and 16 as

$$P(t_D) = 0.5 \ (\text{Ln } t_D + 0.8091) \quad (20)$$

It is important to note that Equations 19 and 20 do not take into account the skin factor. Equations 14 and 20 are the most common solutions to the diffusivity equation for the production case in dimensional and dimensionless forms, respectively. For the case of the total drawdown-buildup period and using the Superposition Theorem, the resulting expression is written as

$$(2\pi kH/wv\mu) \ [P_i - P_{ws}] = P_D(t_D + \delta t_D) - P_D(\delta t_D) \quad (21)$$

Employing 20 and the dimensionless time definition

$$(2\pi kH/wv\mu) \ [P_i - P_{ws}] = 0.5 \text{ Ln } [(t+\delta t)/\delta t] \quad (22)$$

Rearranging and changing the logarithmic base in Equation 22

$$P_{ws} = P_i - 0.1832 \ (wv\mu/kH) \text{ Log } [(t+\delta t)/\delta t] \quad (23)$$

On semilog paper, this equation describes a straight line with slope

$$m = 0.1832 \ (wv\mu/kH) \quad (24)$$

Now, substituting P_i from Equation 18 into Equation 23 and solving for s

$$s = 1.1513 \ [(P_{ws}(t=1) - P_{wf}(\delta t=0))/m + \text{Log } ((t_p+1)/t_p) - \text{Log } (k/(\phi C_t \mu r_w^2)) - 0.3513] \quad (25)$$

Equations 23 and 25 are the basic expressions in the interpretation of buildup tests.

6.3.2. Distance to sealing fault

For pressure buildup testing, Earlougher (1977) used the intersection of the late time two straight lines and relates it to the dimensionless pressure, at the intersection time by

$$P_D(t_D/(2L/r_w^2)) = 0.5 \text{ Ln } [(t_p+\delta t)/\delta t]_x \qquad (26)$$

Thus, to estimate the distance to a linear fault, one finds $[(t_p+\delta t)/\delta t]$ when the semilog straight lines intersect and calculate P_D from equation 26. From Figure 22 of the Earlougher monograph with that value of P_D and the value of $(t_D/(2L/r_w^2)$ is found, where finally

$$L = \sqrt{[kHt_p/4\phi C_t H\mu(t_D/(2L/r_w^2))]} \qquad (27)$$

6.3.3. Double-porosity reservoir

Deruyck et al. (1982) present the theory for double-porosity behaviour which can be applied to both naturally fractured and multilayered reservoirs. The diffusivity equation for the fissured medium according to the terminology of Gringarten (1982) becomes

$$k_f/\mu \ \nabla^2 P_f = (\phi VC_t)_f \ \delta P_f/\delta t - q^* \qquad (28)$$

The counter part equation for the matrix medium can be written

$$k_m/\mu \ \nabla^2 P_m = (\phi VC_t)_m \ \delta P_m/\delta t + q^* \qquad (29)$$

V is the concentration of one medium (i.e. the ratio of that medium to the bulk volume); q^* is the interporosity flow, namely, the flow from the matrix to the fissure. It is assumed in this system of equations, that the reservoir is of infinite lateral extent; with closed top and bottom boundaries; the fluid is slightly compressible; and flow is single phase and laminar; the gravitational forces are negligible; and the pressure gradients are small; the porosity of either medium is independent

of the pressure variations; and finally, the flow to the well occurs via the most permeable medium only, the least permeable medium just acting as a source. Here, the interporosity flow parameter is defined as

$$\lambda = \alpha\ r_w^2\ k_m/k_f \qquad (30)$$

and represents the facility of the fluid to flow from the matrix to the fissure. The ratio of the storativity of the fissure system to the storativity of the total fissure-matrix system is defined

$$\Omega = (\phi VC_t)_f\ /(\ (\phi VC_t)_f + (\phi VC_t)_m\ ) = 10^{-\delta P/m} \qquad (31)$$

where δP is the pressure increment between the two straight lines. For the case of constant flow rate production, the solution in the Laplace space for the fissured part is given by

$$P_{fDL} = k_0\ [\sqrt{(s\ f(s))}\ \ r_D]/\ (\ s\sqrt{(s\ f(s))}\ \ k_1[\sqrt{(s\ f(s))}\ ] \qquad (32)$$

where

$$f(s) = (\ \Omega(1-\Omega)s + \lambda\ )/(\ (1-\Omega)s + \lambda\ ) \qquad (33)$$

and k_0 and k_1 are the modified Bessel functions of second kind, of zero and first order respectively.

6.4. Estimation of Double-Porosity Parameters

6.4.1. Horner method

From the Horner plot Figure 16, the average reservoir pressure can be estimated, extrapolating the late time straight line, until it intersects the pressure axis. That occurs when $\mathrm{Log}[(t_p+\delta t)/\delta t] \approx 0$, implies that $\delta t \gg t_p$. The late time straight line can be expressed as

$$P(\delta t) = 5.695 - 0.4445 \text{ Log } [(t_p+\delta t)/\delta t]$$

Therefore, the average reservoir pressure becomes

$$P(\infty) = 5.695$$

One can estimate the average temperature in a similar form as for the pressure, however, as one can see in Table 2 or in Figure 10, the temperature stabilizes after 1 hour. This permits the assumption that the average reservoir temperature is 265 °C, in that part of the field. In advance, it is pointed out that the interpretation of this test be based on the thermodynamic state defined by the average pressure and temperature of the reservoir. On this basis, one has from the compressed liquid water part of the steam tables (Keenan et al., 1978), the following data

$h = 1158$ [kJ/kg]
$v = 1.2874$ E-03 [m³/kg]
$\mu = 1.0086$ E-04 [Pa-s]

It is interesting to note that the specific stagnation enthalpy corresponding to this thermodynamic state is lower than that estimated by the James method.

Returning to the Horner plot (Figure 12), the left hand parallel straight line represents the total system, its slope can be calculated as

$$m = (5.34-5.327)/\text{Log}(7.625/11.6) = -0.0713$$

Therefore, the conductivity of the medium using Equation 24 is

$$kH = 0.1832(16.19)(1.2874E-03)(1.0086E-04)/(0.0713)$$

$$= 5.4016 \text{ E-12 [m}^3\text{]} \quad (18000 \text{ [md-ft]})$$

The omega parameter can be evaluated using Equation 31 as

$$\Omega = 10^{-0.07156/0.0713} = 0.1$$

As one can be noted from Equation 25, to estimate the skin factor it is necessary to know the porosity, total compressibility and thickness of the reservoir, which are not available.

Nevertheless, to have some idea about this parameter, the following values were assumed

$$\phi = 0.1$$
$$C_t = 1.865E\text{-}09\ [Pa^{-1}] \quad (1.2859E\text{-}05\ [psi]^{-1})$$
$$H = 50\ [m] \quad (164\ [ft])$$

Therefore P(t=1) can be calculated using the slope m with

$$P(t=1) = P_1 = 5.327 - 0.0713\ Log\ (190801/11.6)$$

$$P_1 = 5.0262$$

Substituting values into Equation 25

$$s = 1.1513\ [(5.0262-5.135)/0.0713 + Log\ (190801/190800) - Log\ (5.4016E\text{-}12/((0.1)(1.0086E\text{-}04)(1.865E\text{-}09)(0.108)^2(50)) - 0.3513\ ]$$

$$s = -5.26$$

To estimate the distance to sealing fault

$$P_D(t_D/(2L/r_w^2) = 0.5\ Ln\ (\ 6\ )_x \approx 0.9$$

Coming into Figure 22 (Figure C.2 in Earlougher, 1977)

$$t_D/(2L/r_w^2) = 2.4$$

so that

$$L = \sqrt{[(5.4016E\text{-}12)(190800) / (4\ (0.1)(1.865E\text{-}09)(50)(1.0086E\text{-}04)(2.4))]}$$
$$\approx 338\ [m] \quad (\ 1108\ [ft]\ )$$

6.4.2. Type-curve

In Figure 17, fitting the pressure buildup data, to the double-porosity type curve of Bourdet et al. (1983), the match point is found

$$t_D/c_D = 110$$
$$P_D = 24.3$$
$$\delta P = 1$$
$$\delta t = 3600\ [s]\ (1\ [h])$$

The following parameters were also determined

$$(c_D\ Exp(2s))_f = 100$$
$$(c_D\ Exp(2s))_{f+m} = 10$$

and

$$\lambda\ Exp(-2s) = 1E\text{-}04$$

Thus, the permeability-thickness (conductivity) of the most permeable system is

$$k_f H = wv\mu/2\pi\ (P_D/\delta P)$$
$$= (16.19)(1.2874E\text{-}03)(1.0086E\text{-}04)(24.3)/\ 2\pi(1E6)$$
$$= 8.13028E\text{-}12\ [m^3] \quad (27000\ [md\text{-}ft])$$

The wellbore storage coefficient

$$c = 2\pi k_f H/\mu\ (\delta t/(t_D/c_D)$$
$$= 2\pi(8.13028E\text{-}12)(3600)/(1.0086E\text{-}04)(110)$$
$$= 1.6756E\text{-}05\ [m^3/Pa] \quad (0.7188\ barrel/psi)$$

the storativity ratio

$$\Omega = (c_D \, Exp(2s))_{f+m} / (c_D \, Exp(2s))_f$$
$$= 10/100 = 0.1$$

Using Equation 31, the storativity of the most permeable system is

$$(\phi V C_t)_f = \Omega \, (\phi V C_t)_{f+m}$$
$$= 0.1 \; (9.325E\text{-}09) = 9.325E\text{-}10 \; [Pa]^{-1}$$

The dimensionless wellbore storage coefficient can be calculated with

$$c_D = c/2\pi r_w^2 (\phi C_t H)_{f+m}$$
$$= 1.6576E\text{-}05/2\pi(.108)^2(9.325E\text{-}09) = 24255.125$$

from

$$(c_D \, Exp(2s))_{f+m} = 10$$
$$s = 0.5 \; Ln \; (10/c_D) \approx -3.9$$

Finally, the lambda parameter is

$$Exp(-2s) = 1E\text{-}04$$
$$\lambda = 1E\text{-}04/Exp(2(3.9)) = 4.0973E\text{-}08$$

7. DRAWDOWN SIMULATION

The basic reservoir parameters from a pressure buildup test were determined using the available reservoir theory and thermodynamic principles. The methods of analysis applied to test data and the computed values of the reservoir parameters are summarized immediately

Analysis Method	kH [m^3] X 1E12	Ω (dimensionless)	P(∞) [MPa]
Horner Analysis	5.4	0.1	5.7
Type-Curve Analysis	8.1	0.1	-

The skin factor, the length to the fault, and the interporosity flow coefficient, respectively, were estimated as

s = 5.3 (Horner method)
s = 3.9 (type-curve)
L = 337.9 (Earlougher method)
λ = 4.1E-08 (type-curve method)

These values were obtained by assuming

ϕ = 10 %
C_t = 1.9E-09 [Pa^{-1}]
H = 50 [m]

where C_t is the liquid water compressibility (Grant et al., 1982) at average reservoir conditions. Thus the product ($\phi C_t H$) of the system, called total system storativity, was assumed as 9.3E-09 MPa^{-1}.

It is of interest to know and compare the ideal behaviour of the bottomhole pressure of a well in both homogeneous and double-porosity reservoirs, under similar conditions of

production to that of well A-18. For this purpose two different computer programs were made.

For the case of a well producing from a homogeneous reservoir, the exponential-integral solution was used as well as the superposition principle. The latter was done because of the necessity to take into account the sealing fault effect, which was substituted for an imaginary well producing at the same flow rate as the producing well.

In the case of a well producing from a double-porosity media, the equations given by Deruyck et al. (1982) and presented through this work, were included in the respective program. It was necessary to employ the Stehfest (1970) algorithm in order to find particular solutions to the fissured system. The superposition principle was also used to create the imaginary well to consider the linear boundary effect.

To be consistent in the drawdown simulation of the well under these two different conditions, the thermodynamic state of the fluid defined by the pressure and temperature at average reservoir conditions was used as well as the mass flow rate of well A-18 (16.2 kg/s). All the parameters obtained from the Horner method were utilized. The distance to sealing fault was that computed with the Earlougher method. To complete the data needed to simulate the well, the flow parameter coefficient λ was that determined from type-curve analysis.

The program and the results of the simulation for the well in a homogeneous reservoir are given in Appendix B, while the program and results of simulation of the well in a double-porosity reservoir are presented in Appendix C. The results for the homogeneous reservoir were plotted against the elapsed time and are shown in Figures 18 and 19. The results for the double-porosity reservoir were plotted against the elapsed time and are shown in Figures 20 and 21. The initial reservoir pressure was not plotted in these figures. Its value can be obtained by extrapolating the left hand straight

lines in Figures 18 and 20 to time zero. It was taken as 5.695 [MPa].

In Figures 18 and 20 (or Figures 19 and 21), it is possible to note at early time that the bottomhole pressure for the case of a well in a homogeneous reservoir decreases faster than the respective pressure for the case of a well in a double-porosity media. At later time, the bottomhole pressure declines smoothly in linear form.

To verify the responses of the simulated well in both reservoirs, it can be observed in Figures 19 and 21 that at early time the bottomhole pressure passes through a straight line with slope m. At the time when the boundary effects are felt, the pressure follows another straight with slope 2m.

8. DISCUSSION

The theory presented above was developed considering idealized liquid phase flow. However, the existence of two-phase flow in the drawdown period was pointed out. When the superposition theorem was applied, a constant volumetric flow rate in both periods of the test (production-recovery) was assumed. The viscosity was also considered constant.

A double-porosity reservoir response and a sealing fault effects were detected in the pressure buildup test interpretation.

The simulation of an idealized well producing under similar conditions to that well A-18 from a double-porosity liquid reservoir was carried out for illustration purposes. However, the computed values of the bottomhole pressure for this mass flow rate (16.2 kg/s) can be considered valid within reasonable limits for a short production period. This assumption is based on a boiling front close to the well. Under shut-in conditions single liquid phase is found in the reservoir. For the specific production of well A-18 during the pressure test the induced boiling front was located inside the reservoir, as noted in the heat content increment in the output characteristic of Table 1. It is noted that the boiling front travels into the reservoir according to the extracted mass flow rate, so that for small flow rates as that produced for well A-18, the boiling front was located close to the well.

The simulation of this well for long time periods must be carried out using a more complex model (Grant et al., 1982) which includes relative permeability effects, two-phase compresibilities and rock heat transfer to the fluid.

9. CONCLUSIONS

1. Well A-18 produces from a single medium conductivity fracture located between 1200 and 1250 m depth at 265 °C.

2. During the buildup test interpretation, it was possible to identify a double-porosity response

3. The late time data lie on a semilog straight line with a slope twice the total system slope. It was interpreted as a sealing fault boundary

4. Although the well produced from the reservoir two-phases flow during the drawdown pressure period of the test, the single phase theory seems to be applicable for short time periods within reasonable limits

5. More complex models must applied to represent the phenomena of two-phase flow in the reservoir for both single-well and overall reservoir

ACKNOWLEDGEMENTS

My thanks to the Gerencia de Proyectos Geotermoeléctricos of the Comisión Federal de Electricidad (C.F.E.) de México for the permission to attend the specialized course in Iceland; to the UNU Geothermal Training Programme to accept my participation; to Jón-Steinar Gudmundsson for supervising this work; to my wife Atzimba América Franco de Sánchez and my son Pedro Armando Sánchez Franco for their moral support through this time, and finally; to my family and friends for their appreciable interest.

NOMENCLATURE

A = head of water measured at the weir box [m]
C = compressibility [1/Pa]
c = wellbore storage [m^3/Pa]
D = diameter [m]
H = reservoir thickness [m]
h = specific enthalpy [kJ/kg]
k = permeability [m^2]
L = length to sealing fault [m]
m = slope
P = absolute pressure [MPa]
q = volumetric flow rate [m^3/s]
q^x = interporosity flow [1/s]
r = radial distance [m]
s = skin factor (dimensionless)
T = temperature [°C]
t = time [s]
V = concentration of medium (dimensionless)
v = specific volume [m^3/kg]
w = mass flow rate [kg/s]
X = steam fraction (dimensionless)
α = geometrical factor (dimensionless)
δ = increment or derivative or distance
Γ = Euler constant (0.57721)
λ = interporosity flow coefficient (dimensionless)
μ = viscosity [Pa·s]
∇ = operator nabla
Ω = storativity ratio (dimensionless)
ϕ = porosity (dimensionless)

SUBSCRIPTS

$_0$ = stagnation
$_1$ = taken at t=1
$_c$ = critical
$_D$ = dimensionless
$_d$ = discharge

$_f$ = most permeable media

$_i$ = initial

$_l$ = liquid water

$_m$ = least permeable media

$_p$ = production

$_s$ = steam

$_t$ = total

$_x$ = intersection

$_{wf}$ = bottomhole (flowing)

$_{ws}$ = bottomhole (static)

$_{wh}$ = wellhead

REFERENCES

Alonso, H.: "Current Perspectives on the Development of Geothermics in México," EPRI/IIE Geothermal Conference and Workshop, June 25-28, 1985, San Diego, California, U.S.A.

Ambastha, A.K. and Gudmundsson, J.S.: "Geothermal Two-Phase Wellbore Flow: Pressure Drop Correlations and Flow Pattern Transitions," Proceedings Eleventh Workshop on Geothermal Reservoir Engineering, Stanford University, Stanford, California, January 21-23, 1986, SGP-TR-93.

Ambastha, A.K. and Gudmundsson, J.S.: "Pressure Profile in Two-Phase Geothermal Wells: Comparison of Field Data and Model Calculations," Proceedings Eleventh Workshop on Geothermal Reservoir Engineering, Stanford University, Stanford, California, January 21-23, 1986, SGP-TR-93.

American Society of Mechanical Engineers (ASME): "Fluid Meters, Their Theory and Application," 1971, New York, U.S.A.

Bourdet, D.: "Interpreting in Fractured Reservoirs," World Oil, October 1983.

Dake, L.: Fundamentals of Reservoir Engineering, Elsevier Scientific Publishing Company, 1978.

Deruyck, B., Bourdet, D., Da Prant, G. and Ramey, H.J.: "Interpretation of Interference Tests in Reservoir with Double-Porosity Behaviour-Theory and Field Examples," SPE 11025 (1982).

Earlougher, R.: Advances in Well Test Analysis, Monograph Volume 5, SPE of AIME, Dallas, 1977.

Grant, M., Donaldson, I., and Bixley, P.:Geothermal Reservoir Engineering, Academic Press, 1982.

Gringarten, A.: "Flow Test Evaluation of Fractured Reservoirs," in Recent Trends in Hydro-geology, Geological Society of America, special paper 189, Editor T.N. Narasimhan, 1982, 237-263.

Gringarten, A.:"Interpretation of Transient Well Test Data," Developments in Petroleum Engineering-1, Editors R.A. Dawe and D.C. Wilson, Elsevier Applied Science Publishers, 1985.

James, R.:"Steam-Water Critical Flow Through Pipes to the Atmosphere," Proc.Inst.Mech.,Vol. 176, No.26, 1962.

James, R.:"Gas Content of a Hot Water Reservoir Estimated from Downhole Pressure and Temperature Measurements," Proceedings Second United Nations Symposium on the Development and Use of Geothermal Resources, May 20-29, 1975, San Francisco, California, U.S.A.

Keenan, J., Keyes, F., Hill, P. and Moore, J.: Steam Tables, Wiley-Interscience Publication, John Wiley and Sons, 1978.

Matthews, C. and Russell, D.: Pressure Buildup and Flow Test in Wells, Monograph Volume 1, SPE of AIME, Dallas, 1967.

Molinar, R.: "Recent Activities in Reservoir Engineering at México's Geothermal Fields," EPRI/IIE Geothermal Conference and Workshop, June 25-28, 1985, San Diego, California, U.S.A.

Ortega, L.: "Operation of the Mobile Units of Los Azufres," EPRI/IIE Geothermal Conference and Workshop, June 25-28, 1985, San Diego, California, U.S.A.

Ramey, H., and Gringarten, A.: "Well Tests in Fractured Reservoir," Geothermal Resources Council, Fractures in Geothermal Reservoirs, Special Report no. 12, August 27 and 28, 1982, Honolulu, Hawaii.

Razo, A.: "Geothermal Exploration in México," EPRI/IIE Geothermal Conference and Workshop, June 25-28, 1985, San Diego, California, U.S.A.

Reyes, R.: "Development of the Los Azufres Geothermal Field," EPRI/IIE Geothermal Conference and Workshop, June 25-28, 1985, San Diego, California, U.S.A.

Stehfest, H.: "Numerical Inversion of Laplace Transforms," Communications of the ACM, Volume 13, No. 1, pp 47-49,January, 1970.

TABLE 1. Output curve data
(March, 1986)

Pwh [MPa]	STEAM [kg/s]	WATER [kg/s]	ENTHALPY [kJ/kg]
0.9	25.6	16.6	1764
0.9	25.9	16.8	1763
1.9	25.3	17.5	1728
2.3	20.9	15.9	1676
3.2	6.6	9.6	1314

TABLE 2. Flowing pressure and temperature data
(March 19, 1986)

DEPTH [m]	PRESSURE [MPa]	TEMPERATURE [C]
0	3.236	237.88
100	3.349	241.26
200	3.468	244.47
300	3.591	246.77
400	3.709	248.31
500	3.827	249.99
600	3.958	251.83
700	4.085	253.21
800	4.222	254.90
900	4.358	256.43
1000	4.513	258.43
1050	4.615	259.50
1100	4.734	260.88
1150	4.849	262.13
1200	4.984	263.77
1250	5.282	262.46
1300	5.678	264.43
1320	5.822	266.57

TABLE 3. Pressure and temperature buildup (March 19, 1986)

dt [s]	dt [h]	PRESSURE [MPa]	TEMPERATURE [C]	(tp+dt)/dt (dimensionless)	dp [MPa]
0	0.000	5.135	263.12		0.000
360	0.100	5.271	264.27	531.000	0.136
480	0.133	5.282	264.43	398.000	0.147
600	0.167	5.295	264.43	319.000	0.160
720	0.200	5.299		266.000	0.164
840	0.233	5.303		228.143	0.168
960	0.267	5.307		199.750	0.172
1080	0.300	5.312		177.667	0.177
1200	0.333	5.316		160.000	0.181
1500	0.417	5.320		128.200	0.185
1800	0.500	5.323		107.000	0.188
2400	0.667	5.327		80.500	0.192
3000	0.833	5.332		64.600	0.197
3600	1.000	5.327	264.76	54.000	0.192
4800	1.333	5.323		40.750	0.188
6000	1.667	5.323		32.800	0.188
7200	2.000	5.320	264.76	27.500	0.185
8400	2.333	5.316		23.714	0.181
9600	2.667	5.316		20.875	0.181
10800	3.000	5.316	264.76	18.667	0.181
13200	3.667	5.320		15.455	0.185
15600	4.333	5.323	264.76	13.231	0.188
18000	5.000	5.327	264.76	11.600	0.192
21600	6.000	5.332	264.76	9.833	0.187
25200	7.000	5.336		8.571	0.201
28800	8.000	5.340		7.625	0.205
32400	9.000	5.344	264.76	6.889	0.209
36000	10.000	5.352		6.300	0.217
39600	11.000	5.361	264.76	5.818	0.226
43200	12.000	5.369		5.417	0.234
46800	13.000	5.381	264.76	5.077	0.246
50400	14.000	5.393		4.786	0.258
54000	15.000	5.406	264.76	4.533	0.271
61200	17.000	5.422	264.76	4.118	0.287
68400	19.000	5.438	264.76	3.789	0.303

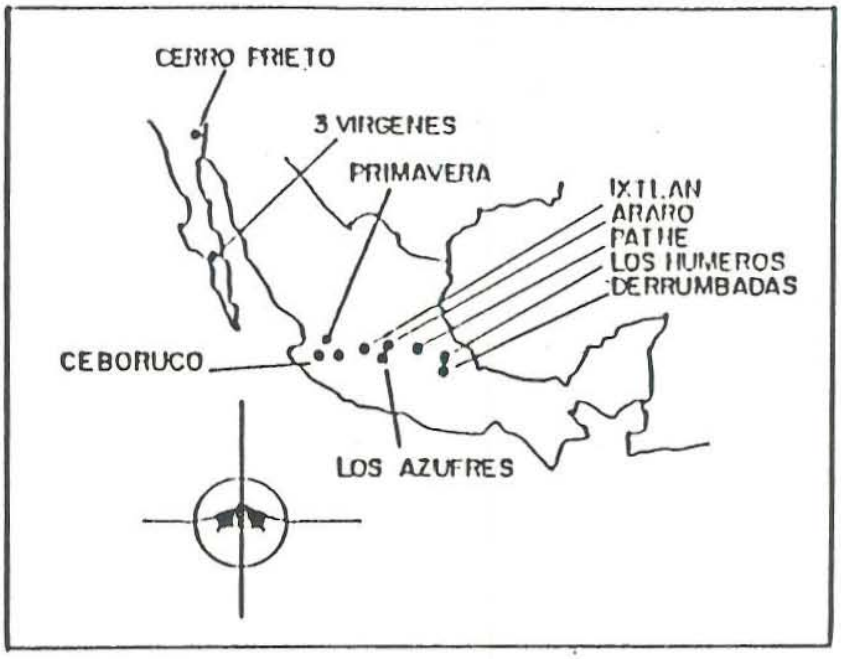

FIGURE 1. MAIN GEOTHERMAL ZONES IN MEXICO

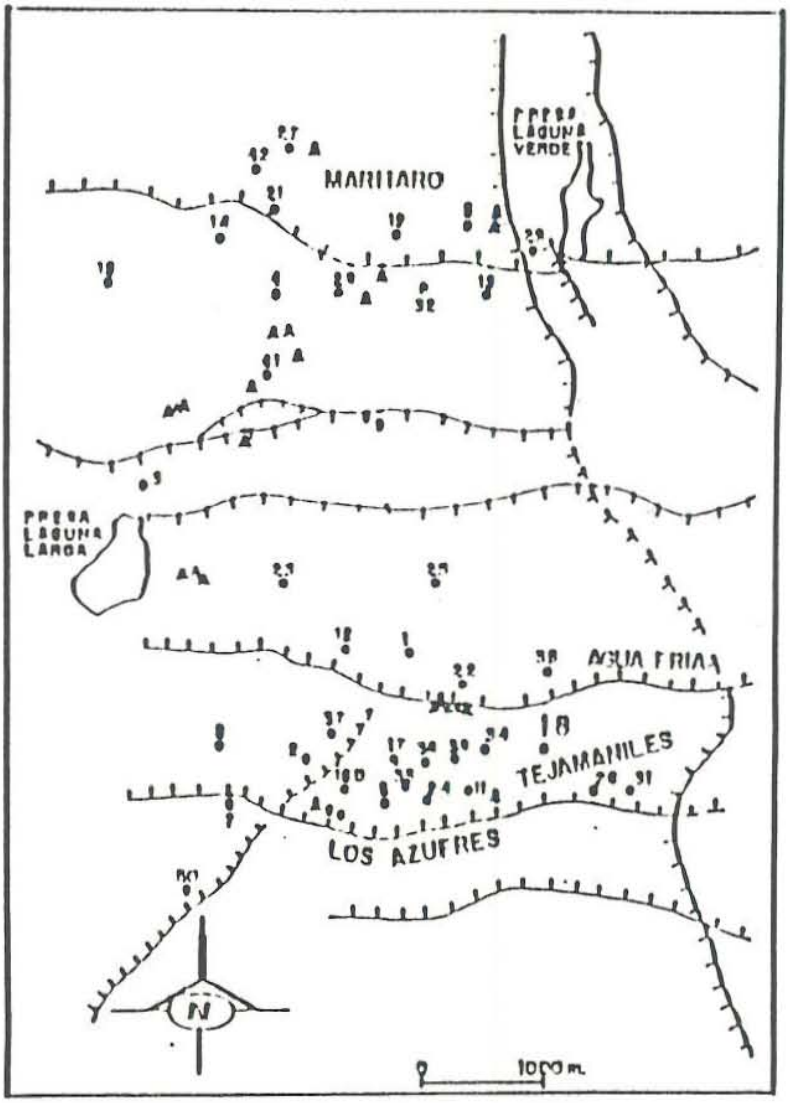

FIGURE 2. LOS AZUFRES GEOTHERMAL FIELD

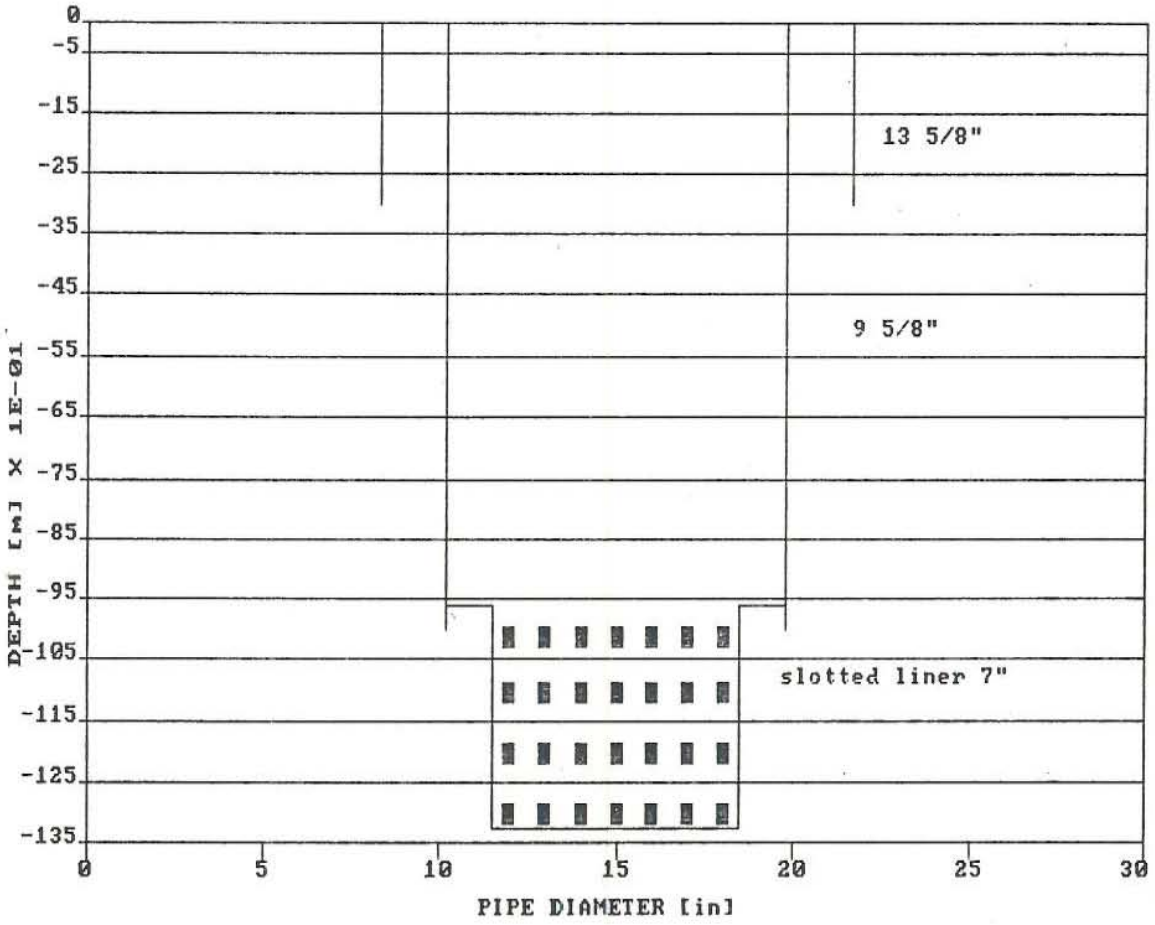

FIGURE 3. WELL COMPLETION

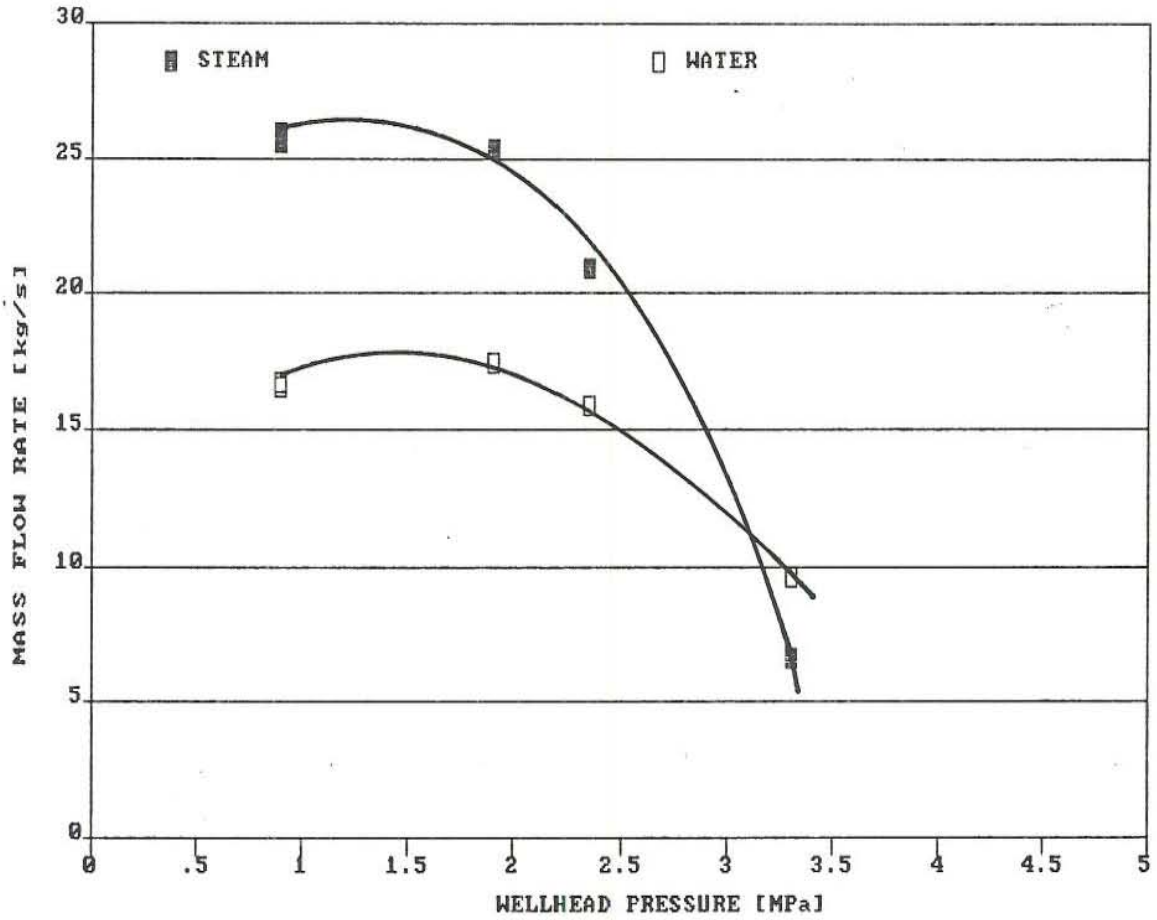

FIGURE 4. OUTPUT CHARACTERISTIC CURVES

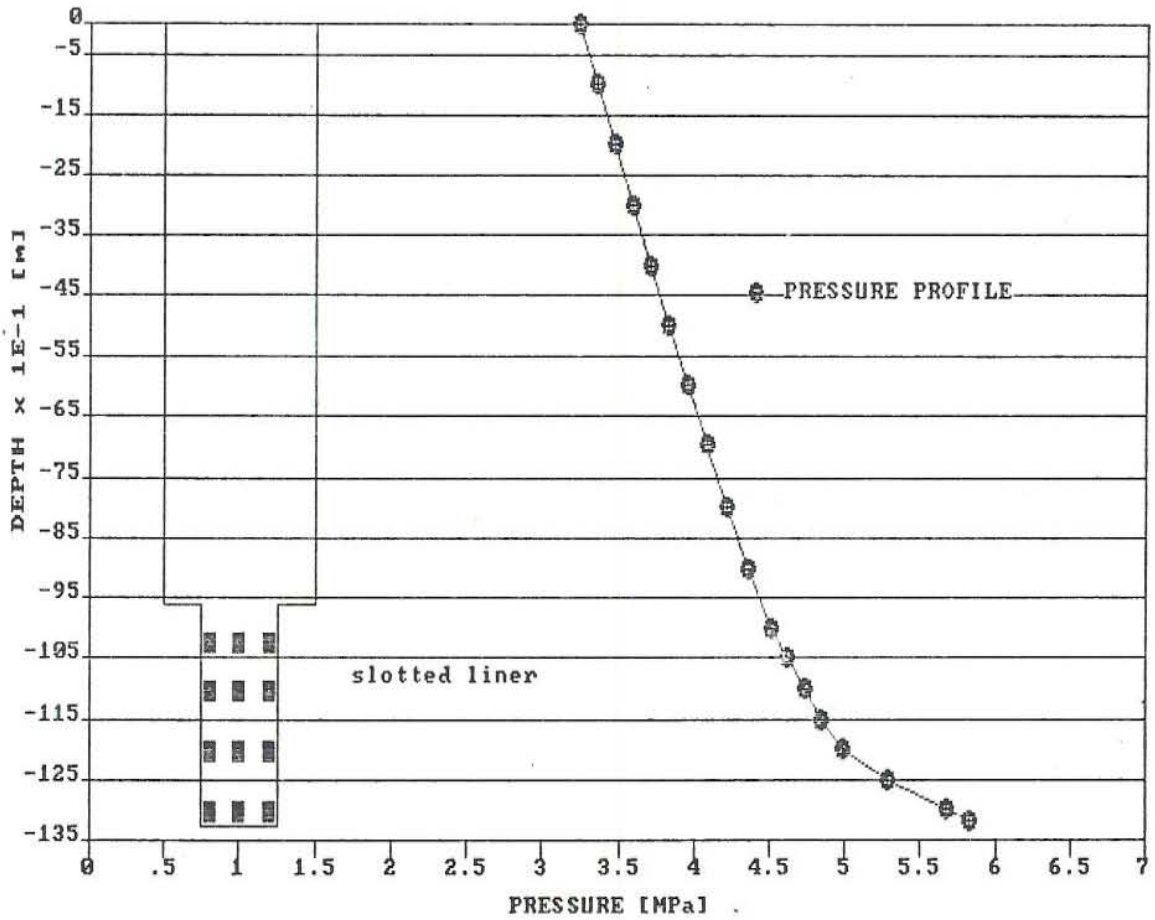

FIGURE 5. FLOWING PRESSURE PROFILE

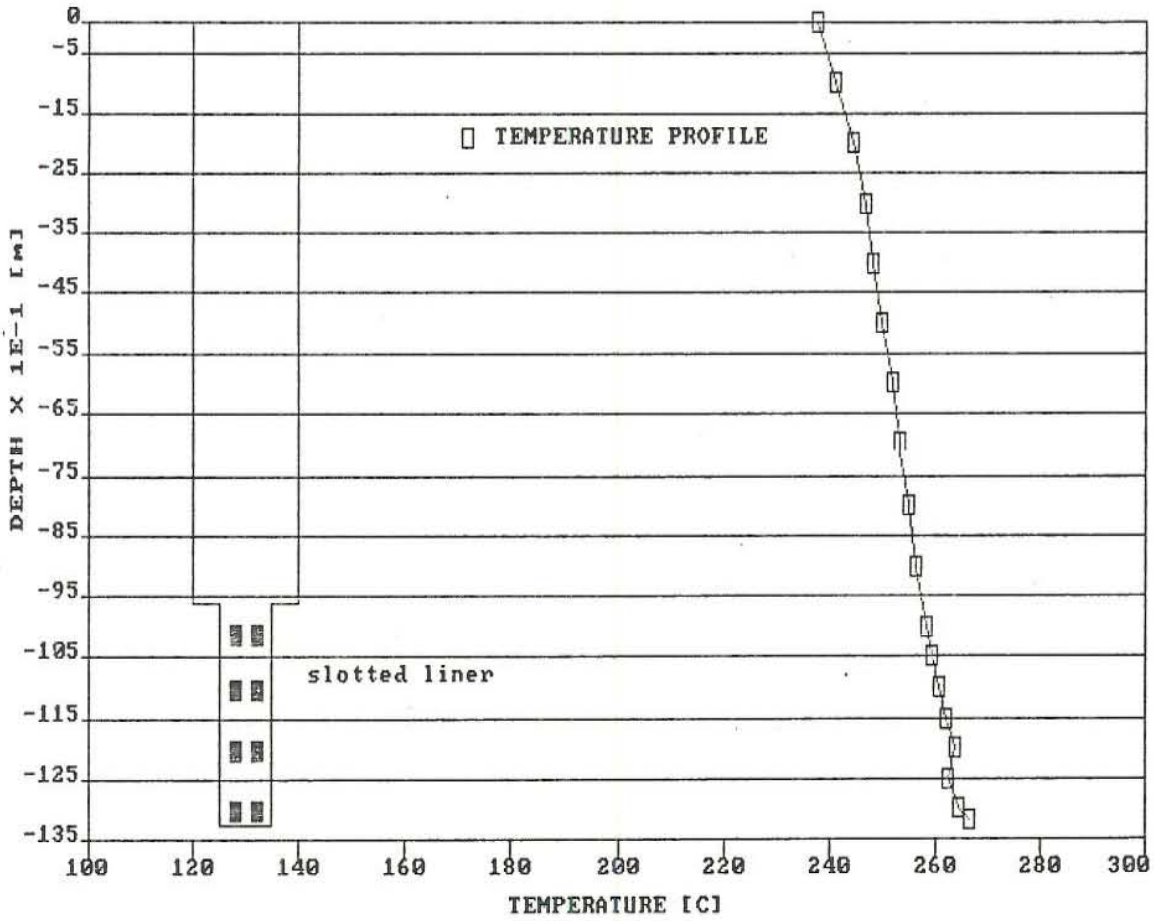

FIGURE 6. FLOWING TEMPERATURE PROFILE

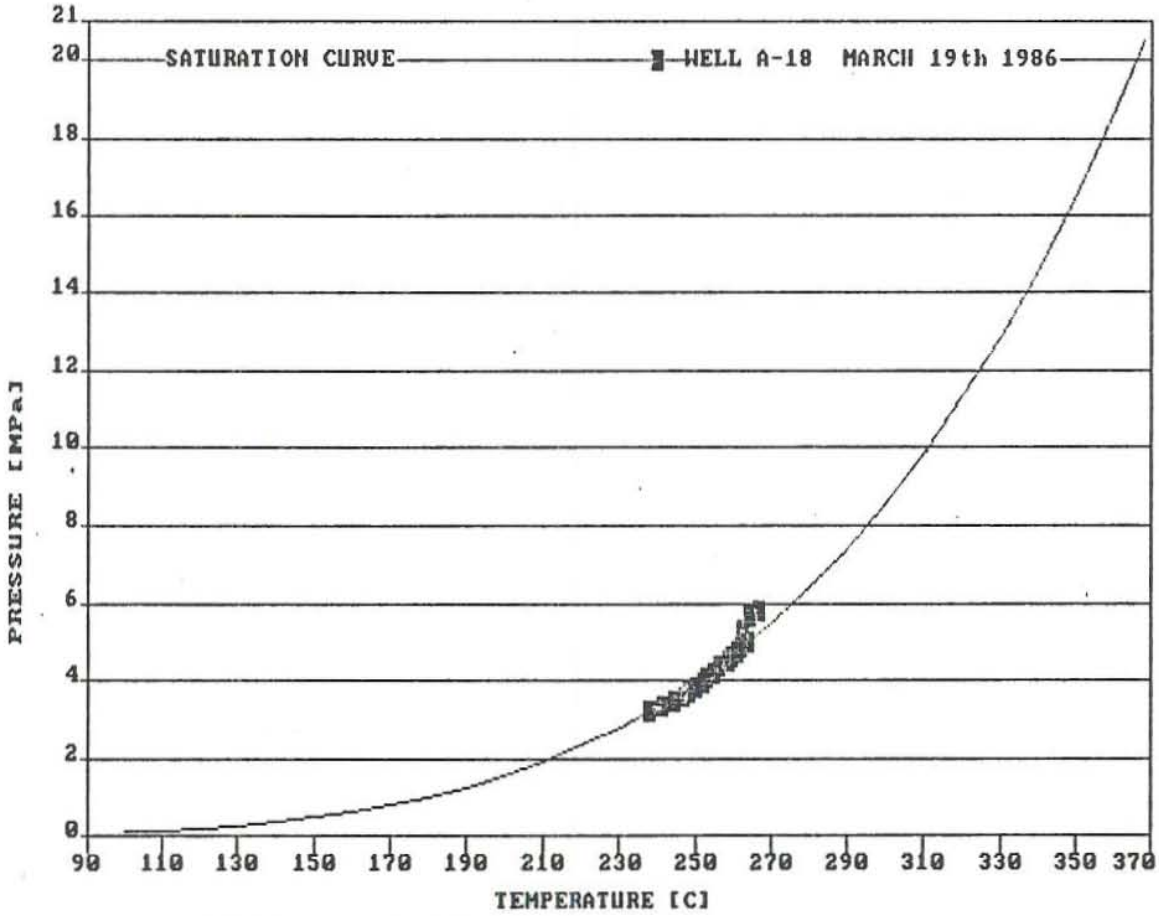

FIGURE 7. THERMODYNAMIC STATES BEFORE SHUT-IN

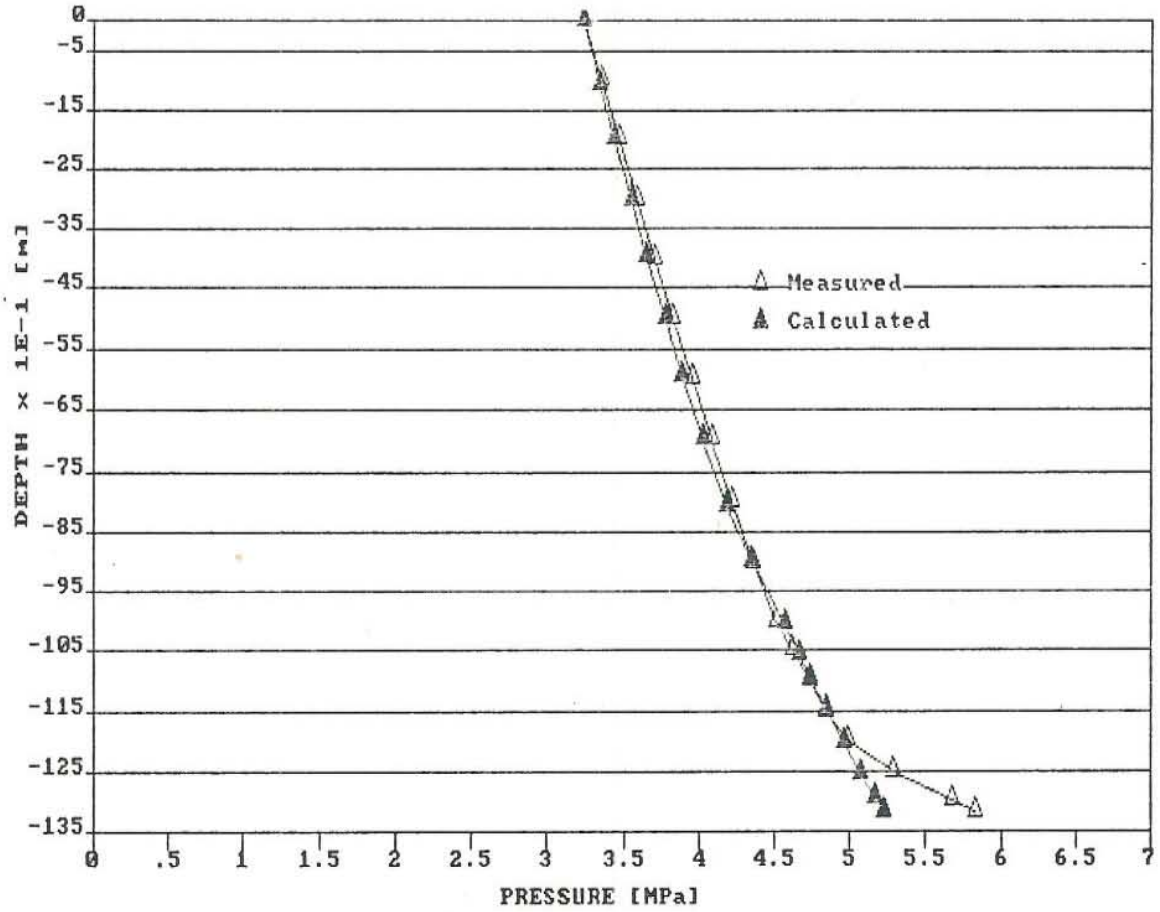

FIGURE 8. COMPARISON BETWEEN MEASURED AND CALCULATED PRESSURE

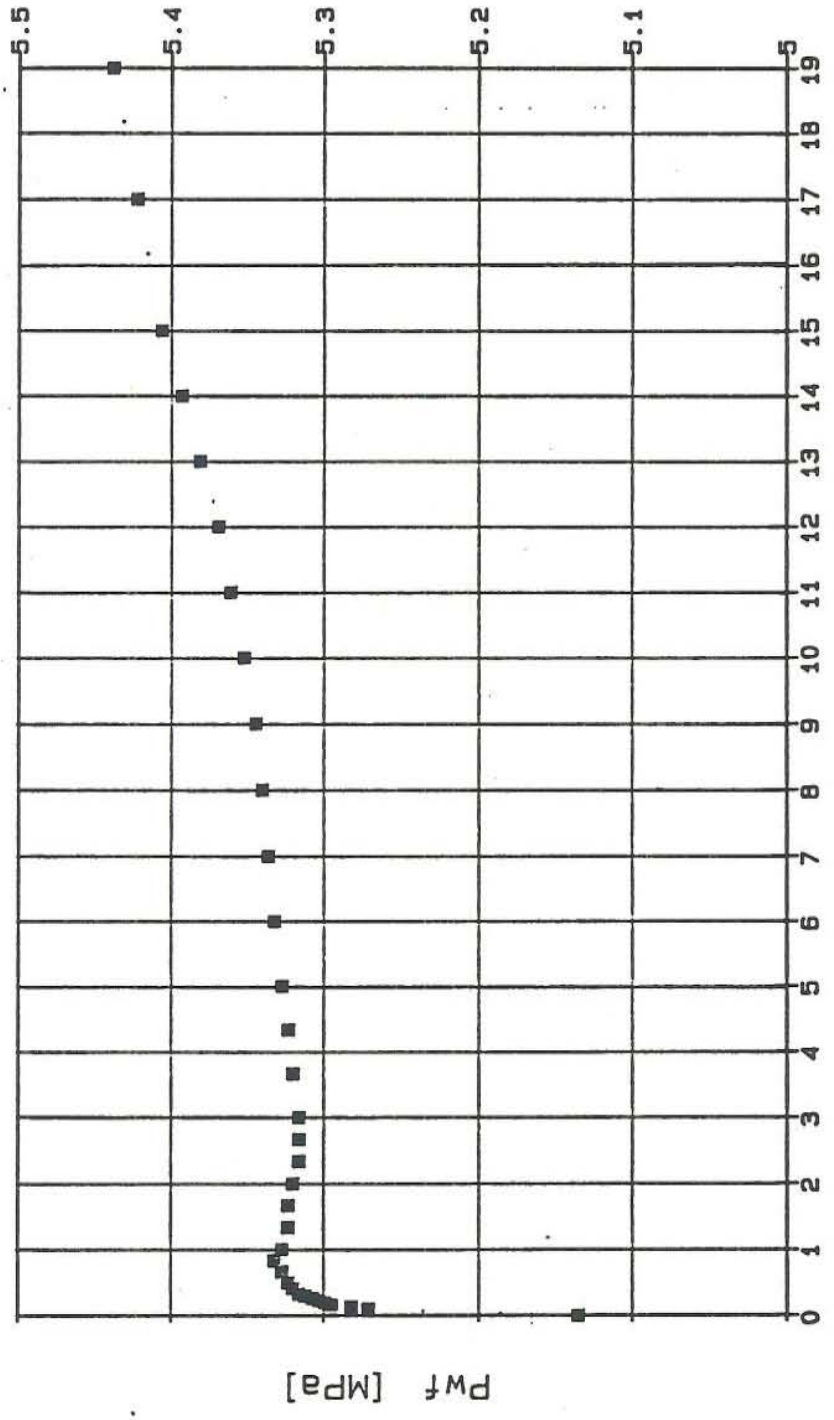

Figure 9. Pressure buildup behavior

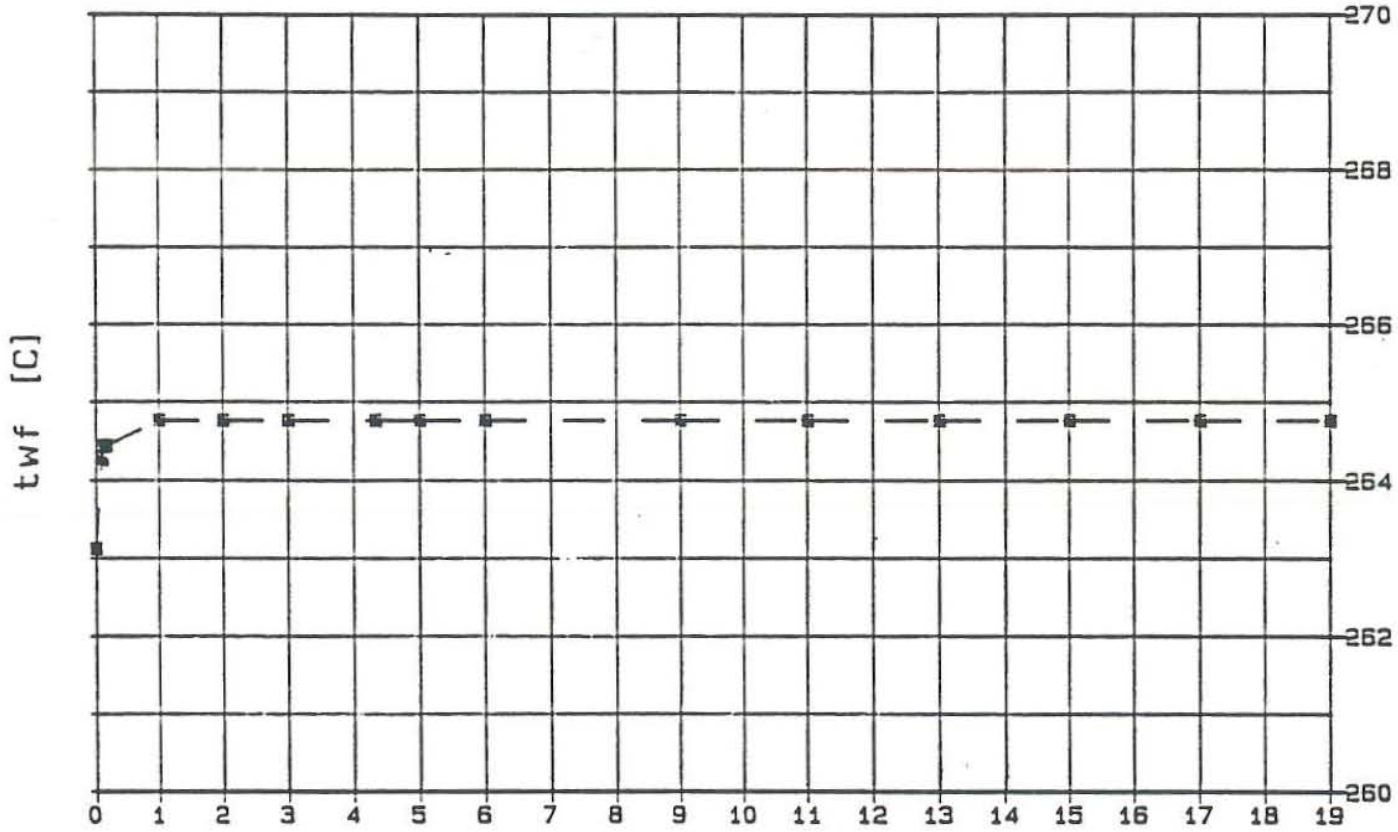

Figure 10. Temperature buildup behavior

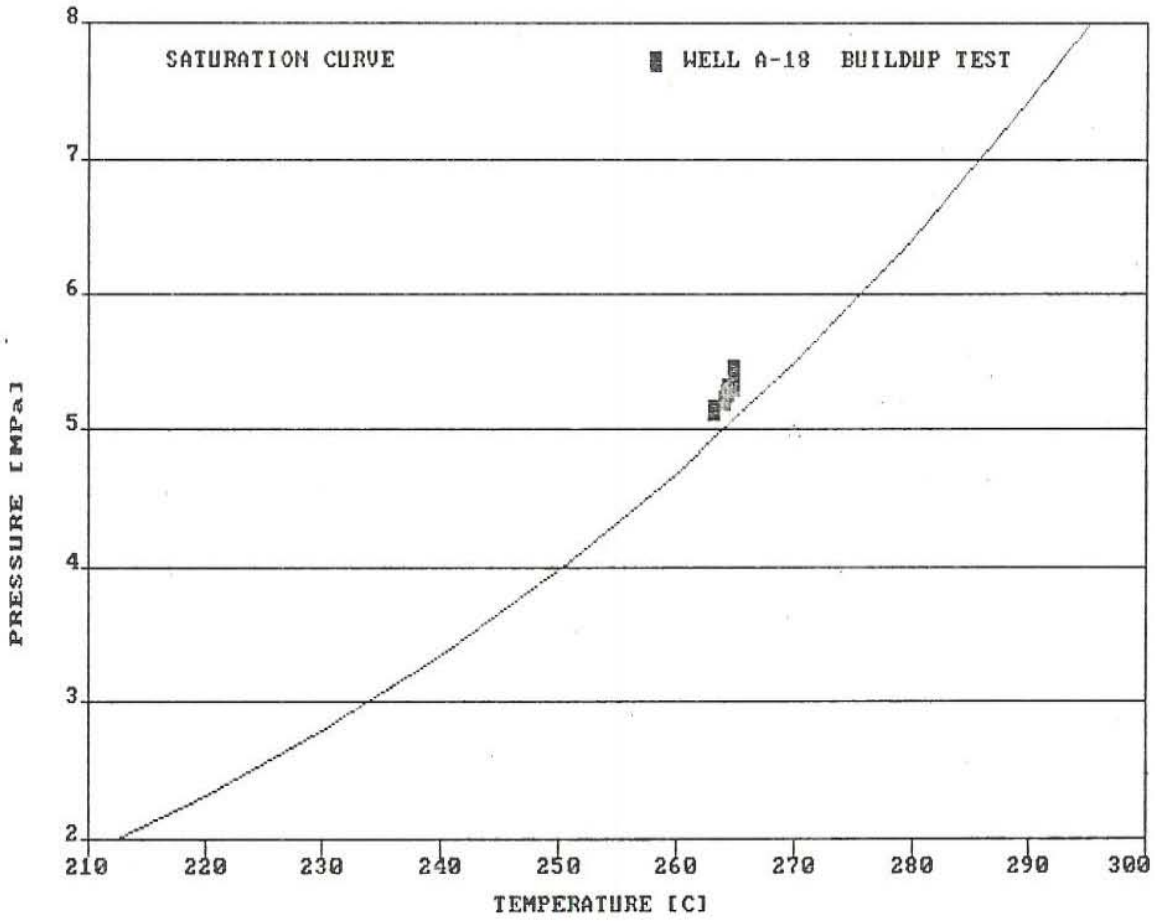

FIGURE 11. THERMODYNAMIC BOTTOMHOLE STATE BEHAVIOR DURING BUILDUP

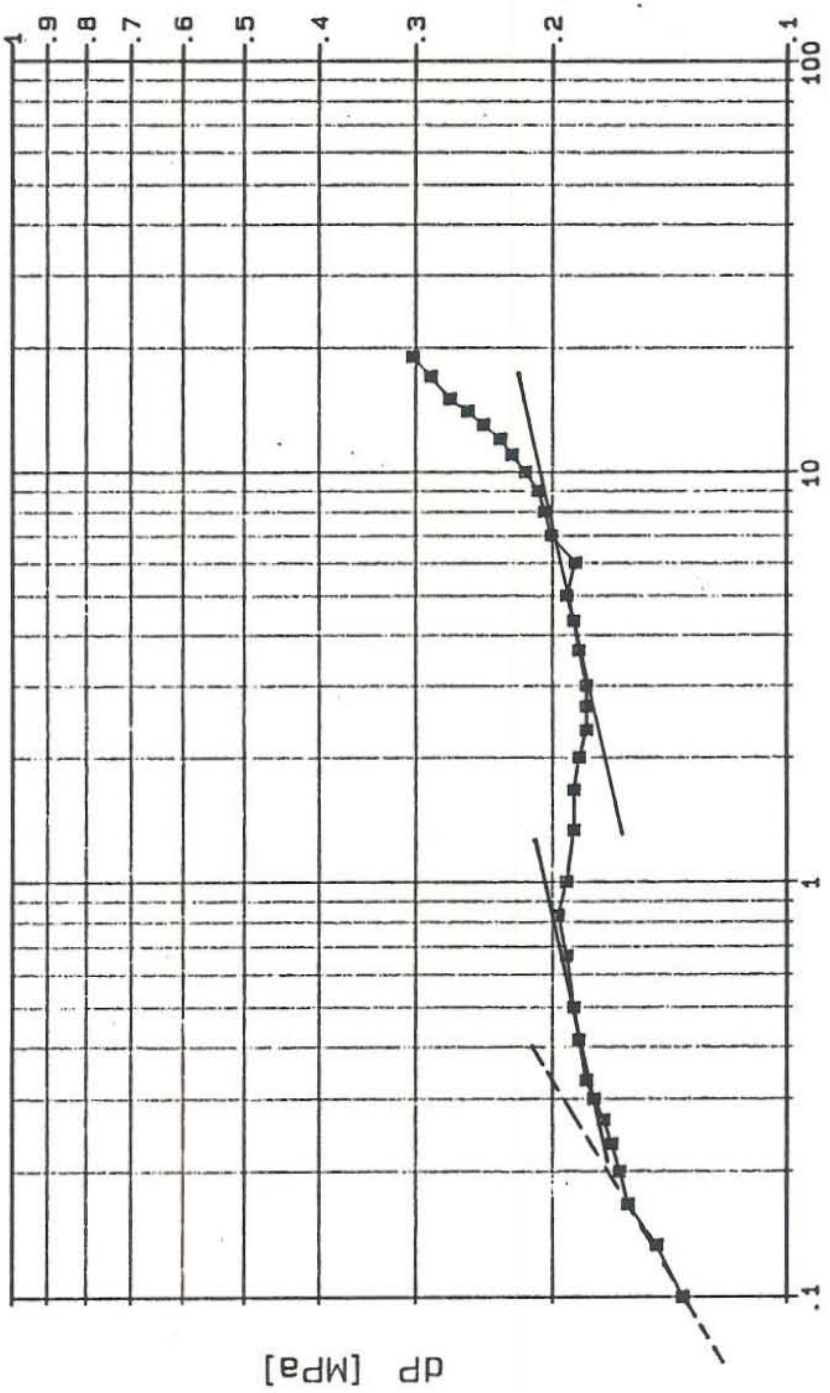

Figure 12. Diagnostic plot

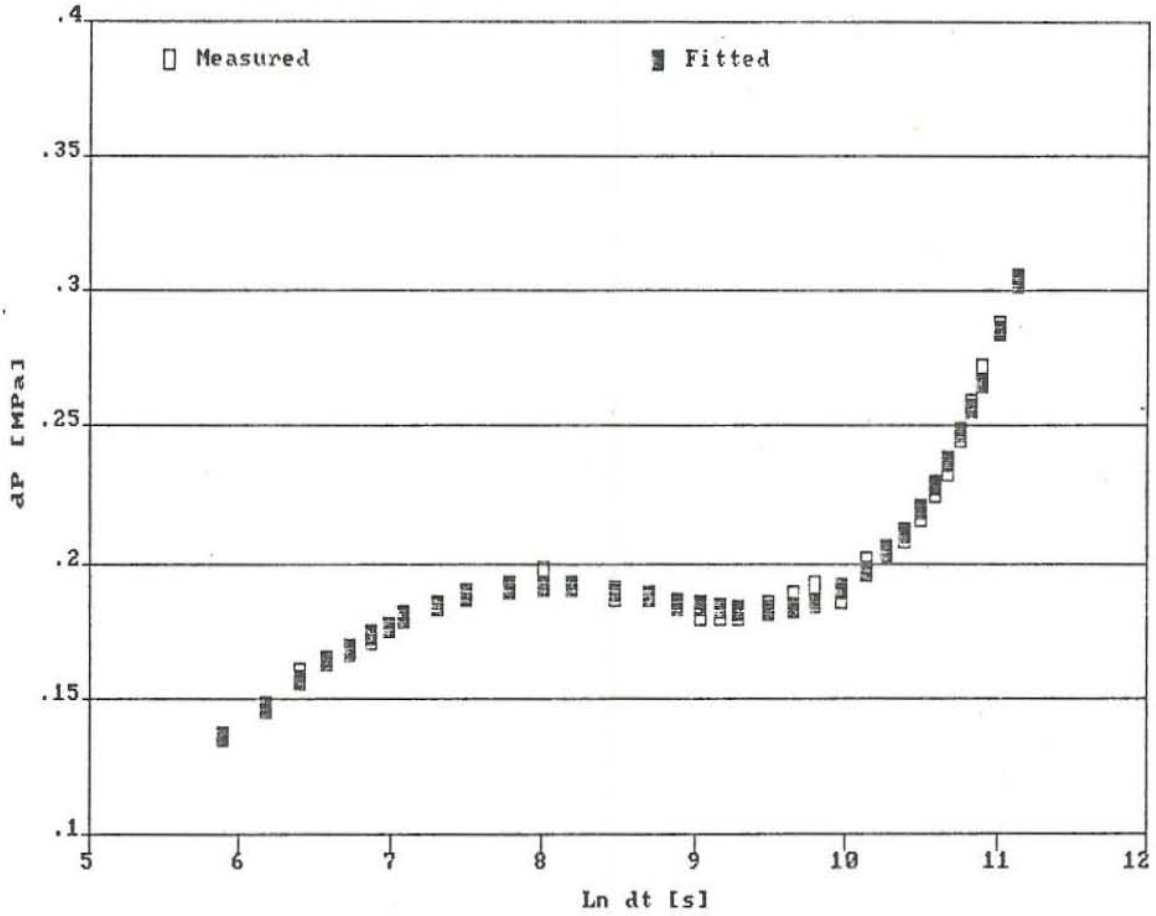

FIGURE 13. COMPARISON BETWEEN MEASURED AND FITTED PRESSURE INCREMENT

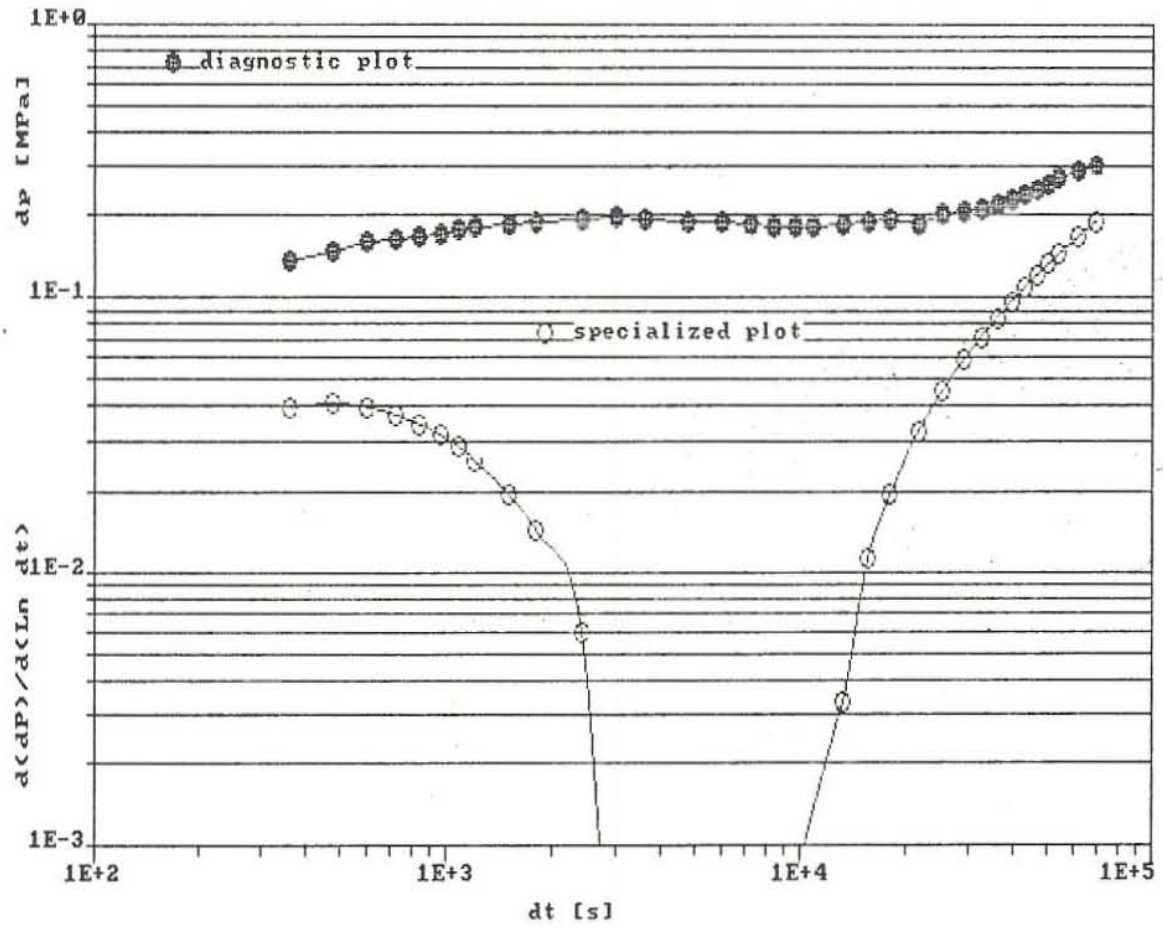

FIGURE 14. DIAGNOSTIC AND SPECIALIZED PLOTS

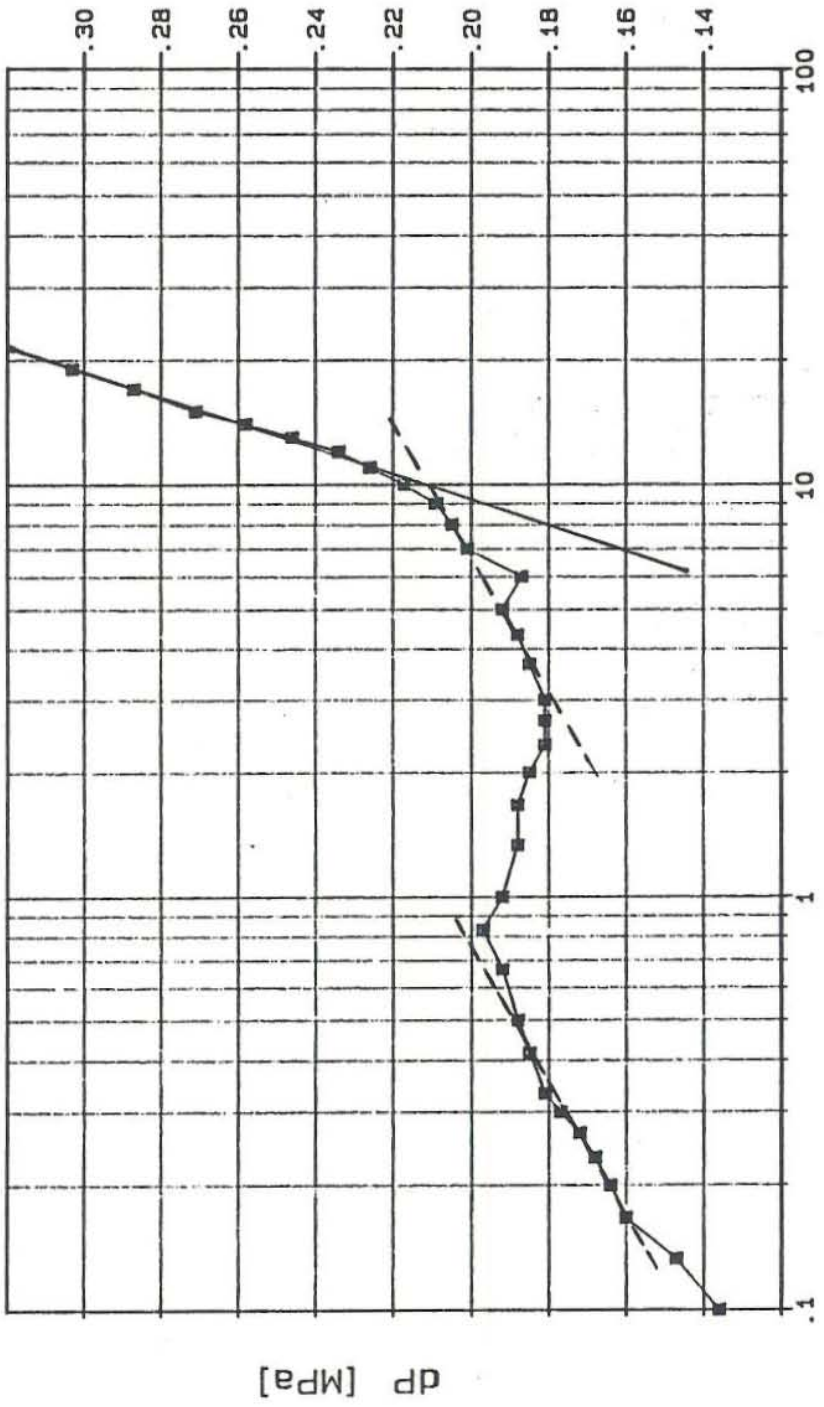

Figure 15. Specialized plot

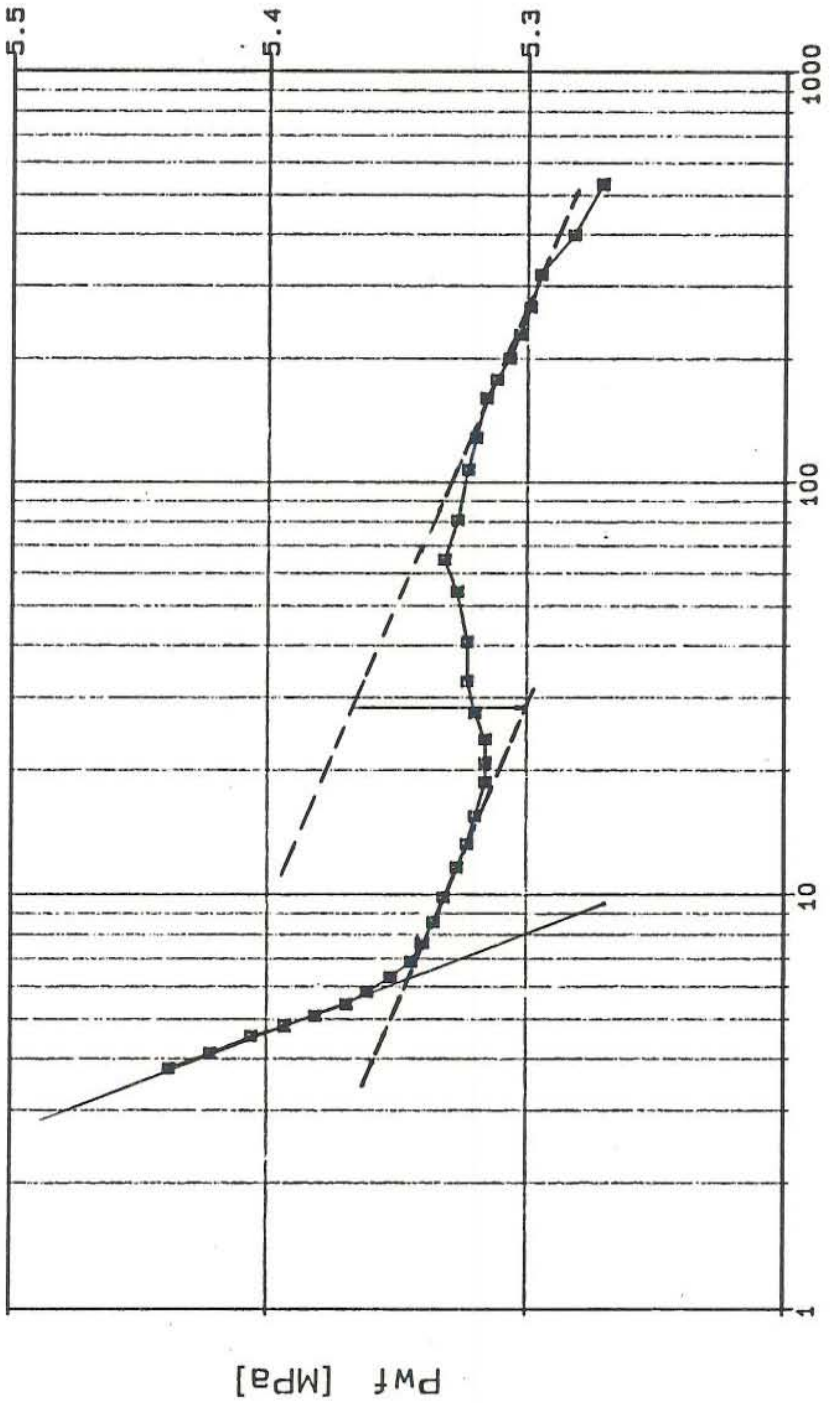

Figure 16. Horner plot

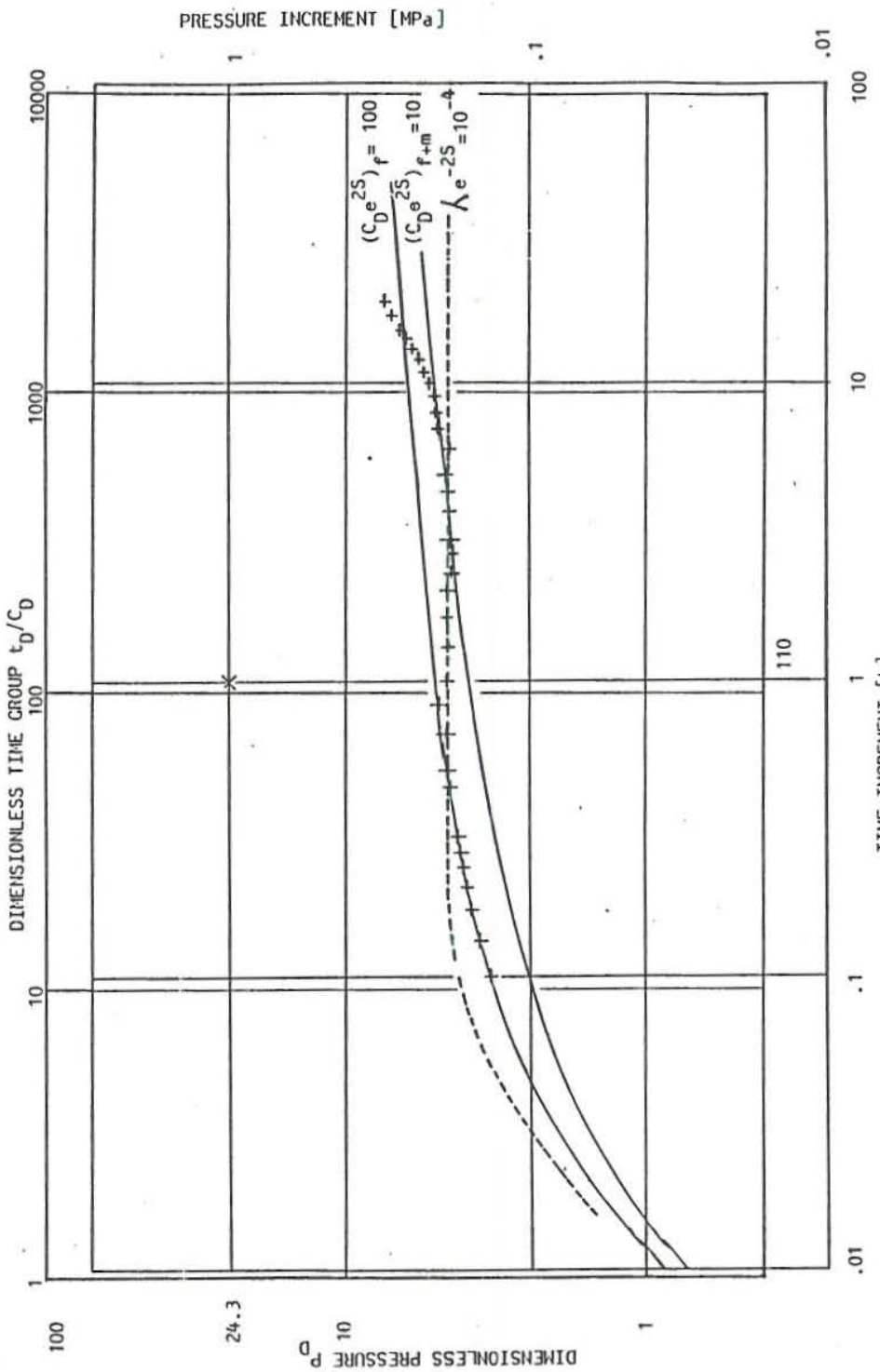

FIGURE 17. FITTING IN A DOUBLE-POROSITY TYPE CURVE

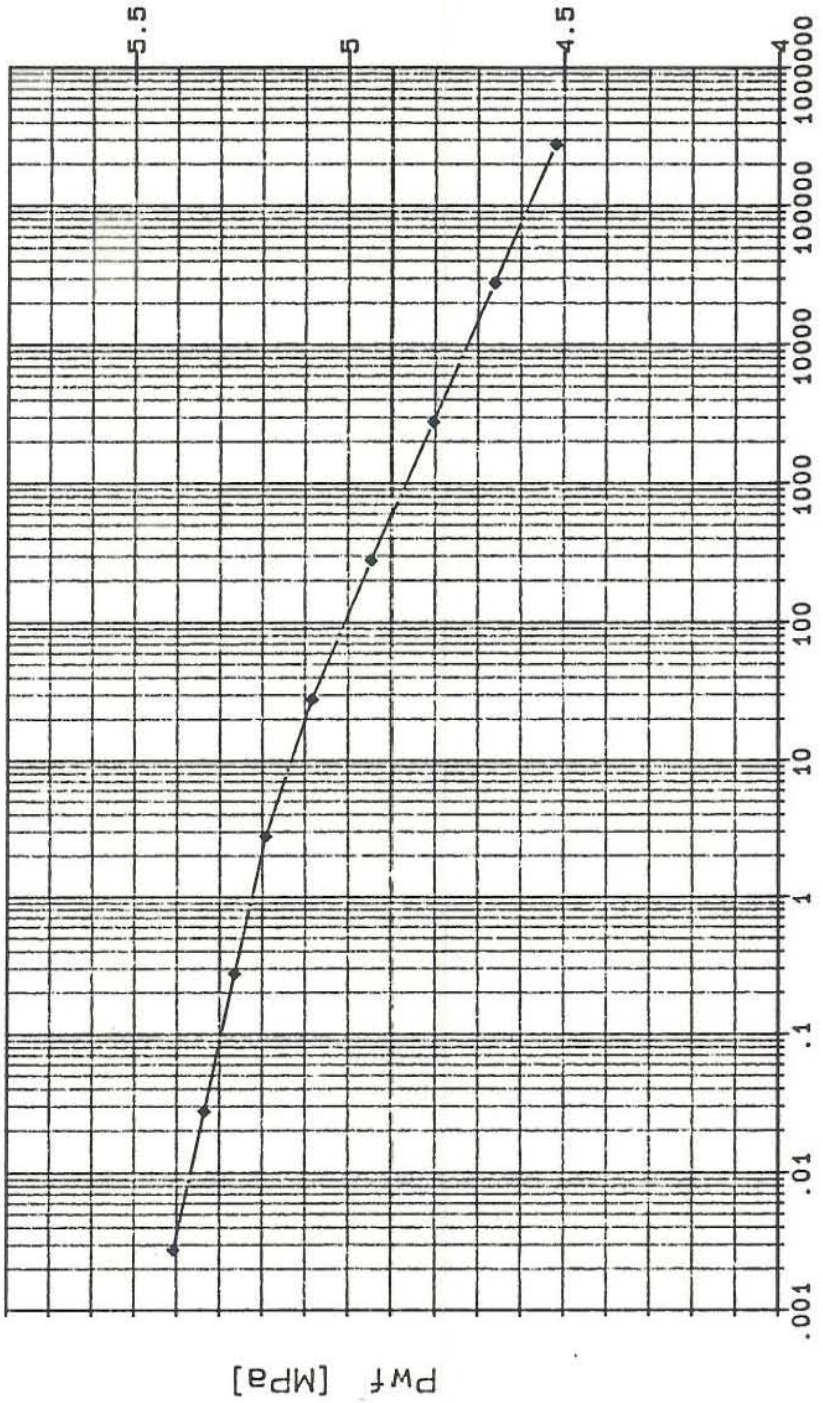

Figure 18. Homogeneous reservoir

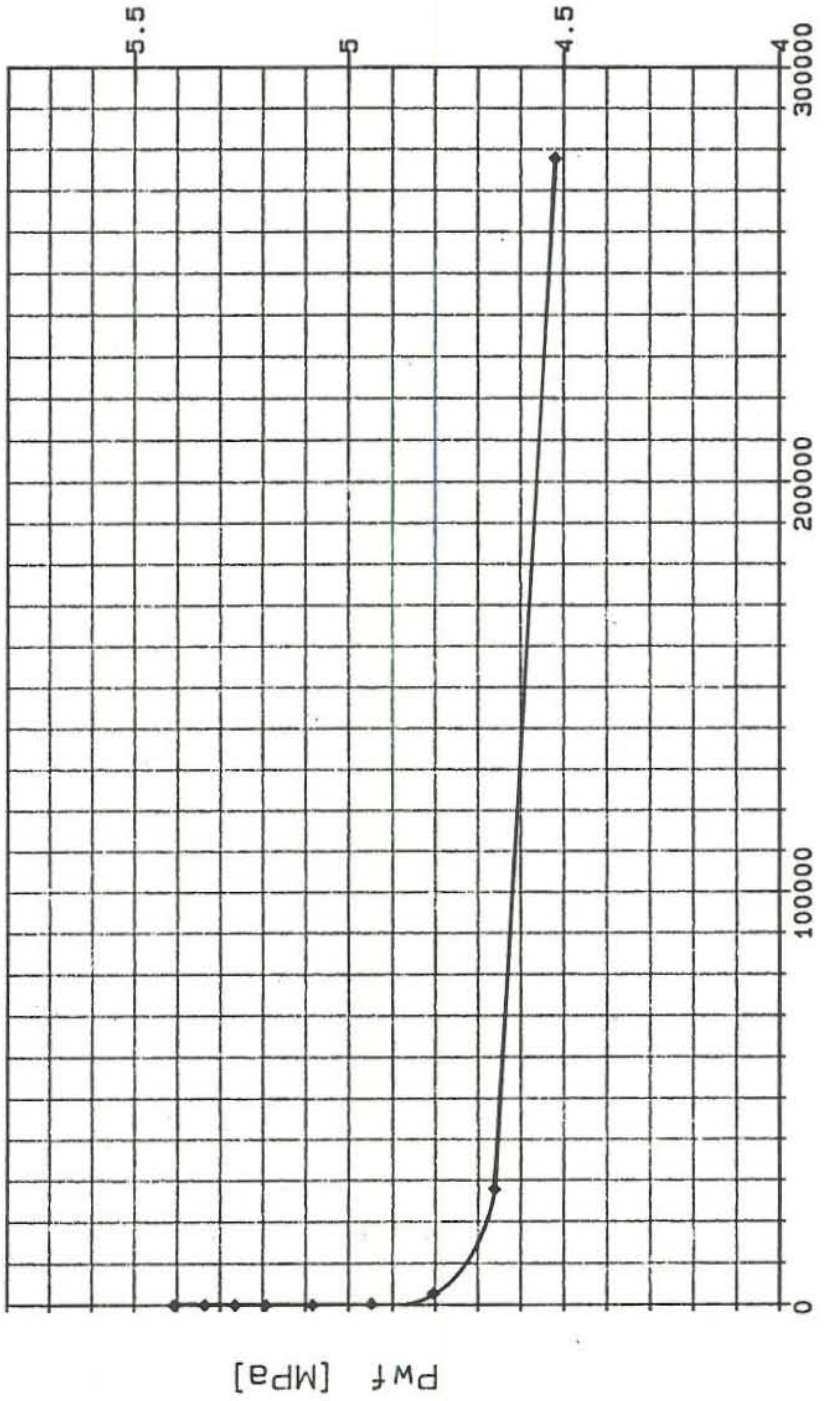

Figure 19. Homogeneous reservoir

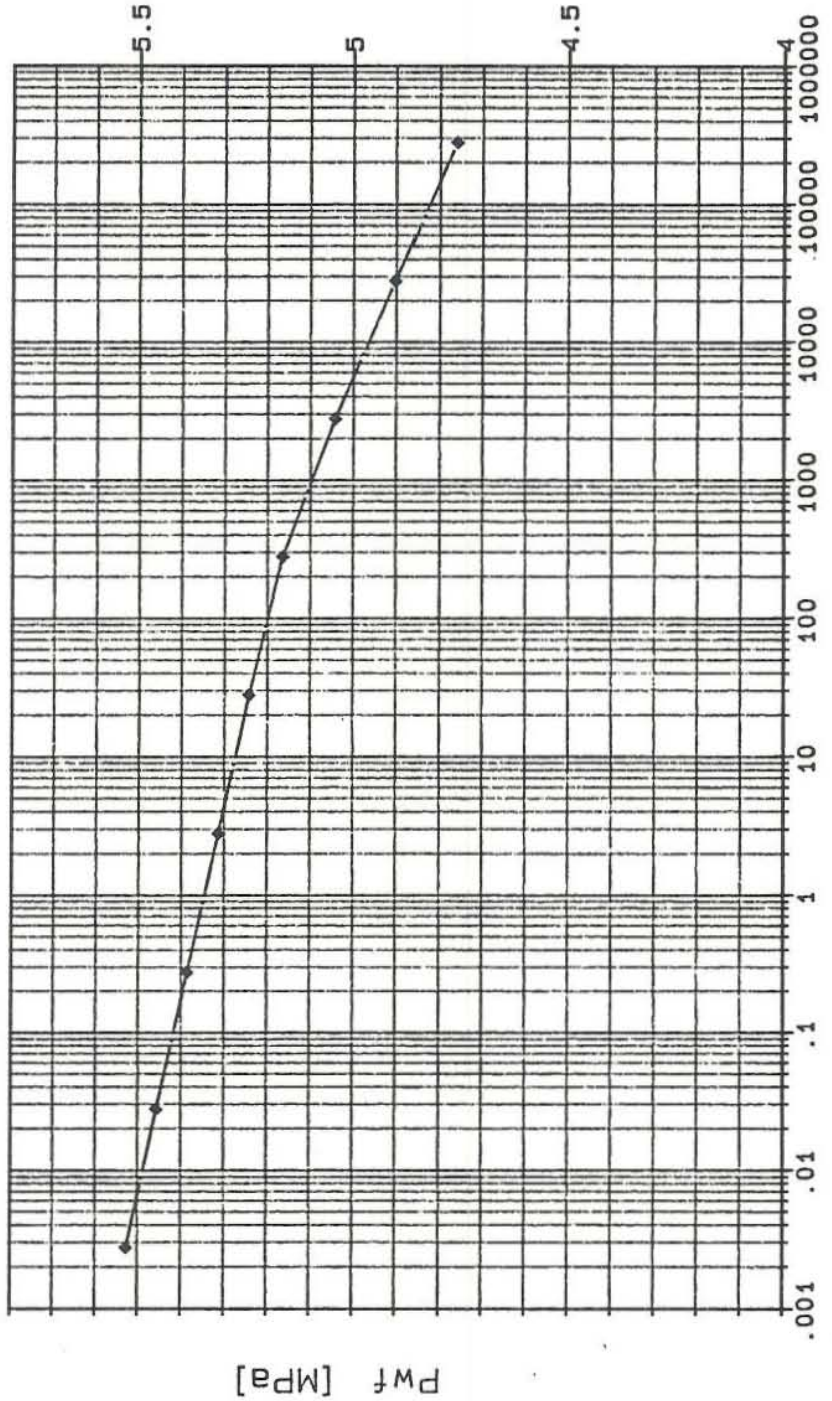

Figure 20. Heterogeneous reservoir

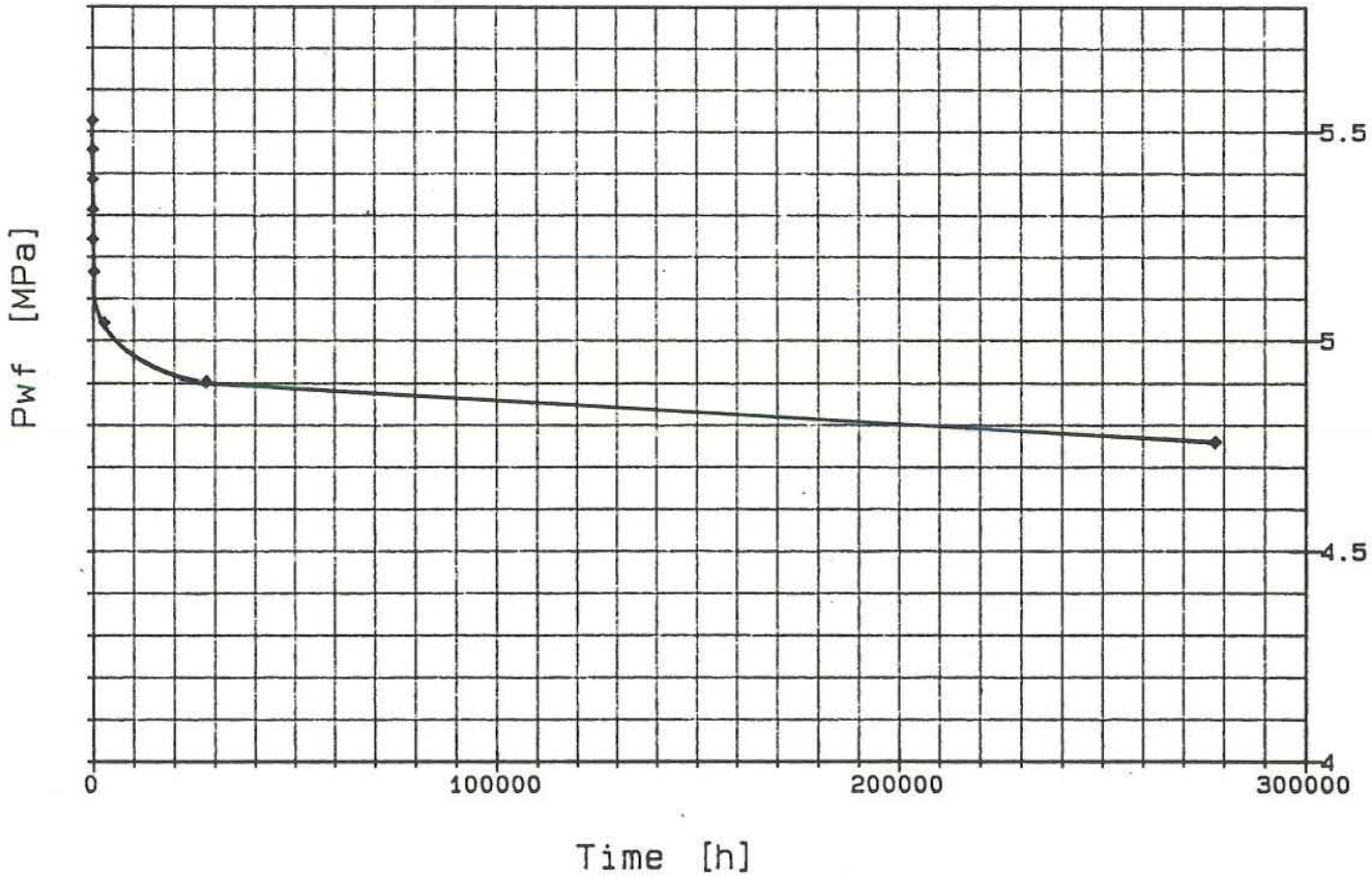

Figure 21. Heterogeneous reservoir

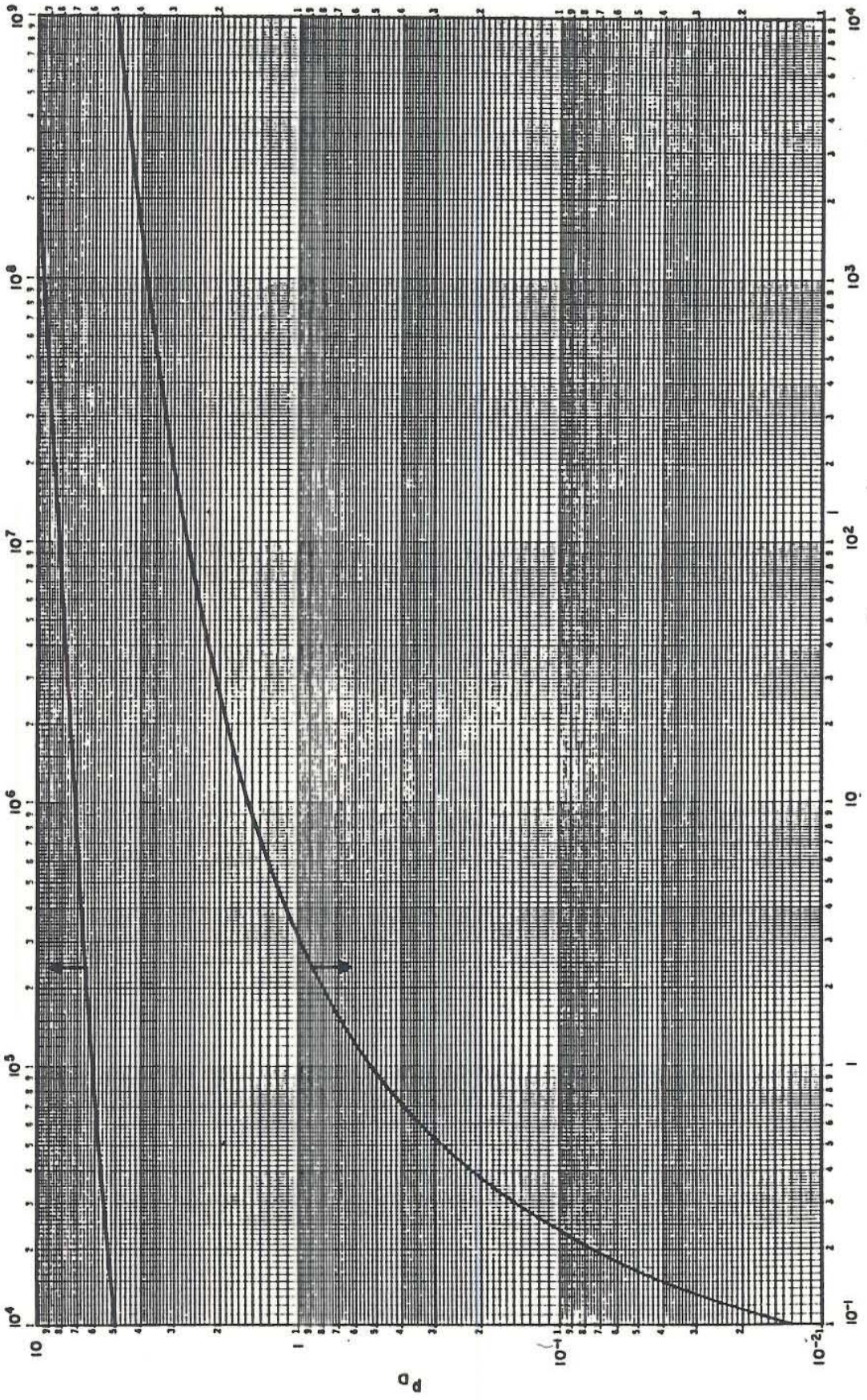

FIGURE 22. Exponential-integral solution

1

Los Azufres well A-18

INPUT DATA AS FOLLOW:

WATER GRAVITY	1.0000
TOTAL MASS FLOWRATE,LB/HR	128516.0000
HEAT TRANSF COEFF,BTU/HR/SQ	0.0000

AT THE WELLHEAD :

DEPTH,FT	0.00
PRESSURE,PSIA	469.30
TEMPERATURE,F	460.62

PIPE DIAMETER USED AS FOLLOW:

FROM 0.0 FT TO 3146.0 FT, PIPE DIAMETER (FT) = 0.7296
ABS ROUGHNESS (FT) = 0.0002

FROM 3146.0 FT TO 4331.0 FT, PIPE DIAMETER (FT) = 0.5153
ABS ROUGHNESS (FT) = 0.0002

TOTAL LENGTH DIVIDED IN 100 INTERVALS

DOWNHOLE SHUT-IN TEMPERATURE AS FOLLOW:

DEPTH,FT	TEMP,F
1640.00	482.00
2297.00	489.00
2953.00	494.00
3445.00	499.00
3773.00	504.00
4101.00	504.00

1

* TWO-PHASE FLOW * DEPTH,FT	PRES,PSIA	TEMP,F	EN,BTU/LB	FRICTION Psi/100ft	ACCELE. Psi/100ft	POTENTIAL Psi/100ft	STM.FRAC	REGIME	qw/A ft/s	qs/A ft/s
0.00	469.30	460.62	565.00				0.1604			
43.31	471.18	461.03	565.00	0.2665	0.0000	4.0810	0.1599	SLUG	1.3867	13.4831
86.62	473.07	461.44	565.00	0.2641	0.0000	4.0958	0.1594	SLUG	1.3880	13.3856
129.93	474.96	461.82	565.00	0.2618	0.0000	4.1095	0.1589	SLUG	1.3892	13.2958
173.24	476.86	462.23	565.00	0.2594	0.0000	4.1242	0.1584	SLUG	1.3904	13.1995
216.55	478.77	462.64	565.00	0.2570	0.0000	4.1389	0.1579	SLUG	1.3917	13.1039
259.86	480.68	463.05	565.00	0.2546	0.0000	4.1537	0.1574	SLUG	1.3930	13.0088
303.17	482.59	463.47	565.00	0.2523	0.0000	4.1684	0.1568	SLUG	1.3943	12.9144
346.48	484.51	463.88	565.00	0.2499	0.0000	4.1831	0.1563	SLUG	1.3956	12.8206
389.79	486.44	464.26	565.00	0.2476	0.0000	4.1979	0.1558	SLUG	1.3969	12.7272
433.10	488.37	464.67	565.00	0.2459	0.0000	4.2198	0.1553	SLUG	1.3981	12.6398
476.41	490.32	465.08	565.00	0.2443	0.0000	4.2476	0.1548	SLUG	1.3994	12.5459
519.72	492.27	465.49	565.00	0.2428	0.0000	4.2763	0.1543	SLUG	1.4007	12.4523
563.03	494.24	465.91	565.00	0.2412	0.0000	4.3047	0.1537	SLUG	1.4020	12.3589
606.34	496.22	466.32	565.00	0.2396	0.0000	4.3337	0.1532	SLUG	1.4033	12.2658
649.65	498.21	466.74	565.00	0.2381	0.0000	4.3628	0.1527	SLUG	1.4046	12.1729

692.96	500.22	467.13	565.00	0.2366	0.0000	4.3903	0.1522	SLUG	1.4050	12.0869
736.27	502.24	467.55	565.00	0.2351	0.0000	4.4203	0.1516	SLUG	1.4072	11.9946
779.58	504.26	467.97	565.00	0.2335	0.0000	4.4503	0.1511	SLUG	1.4085	11.9025
822.89	506.30	468.39	565.00	0.2320	0.0000	4.4810	0.1506	SLUG	1.4099	11.8106
866.20	508.36	468.81	565.00	0.2305	0.0000	4.5118	0.1500	SLUG	1.4112	11.7190
909.51	510.43	469.24	565.00	0.2289	0.0000	4.5429	0.1495	SLUG	1.4126	11.6277
952.82	512.51	469.67	565.00	0.2274	0.0000	4.5741	0.1489	SLUG	1.4139	11.5366
996.13	514.60	470.06	565.00	0.2260	0.0000	4.6041	0.1484	SLUG	1.4152	11.4522
1039.44	516.70	470.49	565.00	0.2245	0.0000	4.6363	0.1479	SLUG	1.4166	11.3616
1082.75	518.82	470.92	565.00	0.2230	0.0000	4.6689	0.1473	SLUG	1.4180	11.2713
1126.06	520.95	471.35	565.00	0.2214	0.0000	4.7015	0.1467	SLUG	1.4194	11.1812
1169.37	523.10	471.78	565.00	0.2199	0.0000	4.7349	0.1462	SLUG	1.4208	11.0914
1212.68	525.26	472.22	565.00	0.2184	0.0000	4.7686	0.1456	SLUG	1.4222	11.0018
1255.99	527.43	472.62	565.00	0.2169	0.0000	4.8027	0.1451	SLUG	1.4236	10.9125
1299.30	529.62	473.06	565.00	0.2155	0.0000	4.8346	0.1445	SLUG	1.4249	10.8295
1342.61	531.82	473.50	565.00	0.2141	0.0000	4.8695	0.1439	SLUG	1.4264	10.7407
1385.92	534.04	473.94	565.00	0.2126	0.0000	4.9044	0.1434	SLUG	1.4278	10.6522
1429.23	536.27	474.38	565.00	0.2111	0.0000	4.9401	0.1428	SLUG	1.4292	10.5639
1472.54	538.51	474.82	565.00	0.2096	0.0000	4.9759	0.1422	SLUG	1.4307	10.4758
1515.85	540.78	475.26	565.00	0.2082	0.0000	5.0125	0.1416	SLUG	1.4321	10.3880
1559.16	543.05	475.68	565.00	0.2068	0.0000	5.0467	0.1411	SLUG	1.4335	10.3063
1602.47	545.34	476.13	565.00	0.2053	0.0000	5.0841	0.1405	SLUG	1.4350	10.2190
1645.78	547.65	476.58	565.00	0.2039	0.0000	5.1216	0.1399	SLUG	1.4365	10.1319
1689.09	549.97	477.03	565.00	0.2024	0.0000	5.1599	0.1393	SLUG	1.4380	10.0451
1732.40	552.31	477.48	565.00	0.2010	0.0000	5.1983	0.1387	SLUG	1.4395	9.9585
1775.71	554.66	477.93	565.00	0.1995	0.0000	5.2372	0.1381	SLUG	1.4410	9.8722
1819.02	557.03	478.39	565.00	0.1981	0.0000	5.2769	0.1375	SLUG	1.4425	9.7861
1862.33	559.42	478.81	565.00	0.1968	0.0000	5.3140	0.1369	SLUG	1.4439	9.7060
1905.64	561.83	479.27	565.00	0.1953	0.0000	5.3547	0.1363	SLUG	1.4454	9.6204
1948.95	564.25	479.73	565.00	0.1939	0.0000	5.3955	0.1357	SLUG	1.4470	9.5350
1992.26	566.68	480.19	565.00	0.1925	0.0000	5.4367	0.1351	SLUG	1.4485	9.4499
2035.57	569.14	480.66	565.00	0.1911	0.0000	5.4789	0.1344	SLUG	1.4501	9.3651
2078.88	571.61	481.12	565.00	0.1897	0.0000	5.5212	0.1338	SLUG	1.4516	9.2805
2122.19	574.10	481.56	565.00	0.1882	0.0000	5.5641	0.1332	SLUG	1.4532	9.1961
2165.50	576.35	481.98	565.00	0.1870	0.0000	5.6098	0.1327	SLUG	1.4546	9.1219
2208.81	578.66	482.41	565.00	0.1703	0.0000	5.1793	0.1321	SLUG	1.4561	9.0454
2252.12	581.06	482.85	565.00	0.1736	0.0000	5.3541	0.1315	SLUG	1.4575	8.9666
2295.43	583.53	483.31	565.00	0.1748	0.0000	5.5329	0.1308	SLUG	1.4591	8.8858
2338.74	586.08	483.78	565.00	0.1799	0.0000	5.7157	0.1302	SLUG	1.4607	8.8032
2382.05	588.72	484.27	565.00	0.1829	0.0000	5.7024	0.1295	SLUG	1.4623	8.7188
2425.36	591.44	484.74	565.00	0.1857	0.0000	6.0931	0.1289	SLUG	1.4640	8.6325
2468.67	594.24	485.25	565.00	0.1883	0.0000	6.2759	0.1282	SLUG	1.4656	8.5497
2511.98	597.12	485.77	565.00	0.1910	0.0000	6.4737	0.1275	SLUG	1.4674	8.4599
2555.29	600.10	486.31	565.00	0.1935	0.0000	6.6756	0.1267	SLUG	1.4692	8.3683
2598.60	603.16	486.87	565.00	0.1959	0.0000	6.8810	0.1260	SLUG	1.4711	8.2750
2641.91	606.32	487.43	565.00	0.1981	0.0000	7.0900	0.1252	SLUG	1.4731	8.1800
2685.22	609.57	488.01	565.00	0.2002	0.0000	7.3024	0.1244	SLUG	1.4751	8.0832
2728.53	612.91	488.58	565.00	0.2020	0.0000	7.5071	0.1236	SLUG	1.4770	7.9900
2771.84	616.34	489.19	565.00	0.2037	0.0000	7.7260	0.1228	SLUG	1.4791	7.8901
2815.15	619.88	489.81	565.00	0.2053	0.0000	7.9481	0.1219	SLUG	1.4813	7.7887
2858.46	623.50	490.45	565.00	0.2067	0.0000	8.1732	0.1210	SLUG	1.4835	7.6858
2901.77	627.23	491.11	565.00	0.2079	0.0000	8.4012	0.1201	SLUG	1.4858	7.5815
2945.08	631.06	491.74	565.00	0.2089	0.0000	8.6320	0.1192	SLUG	1.4881	7.4757
2988.39	634.99	492.42	565.00	0.2096	0.0000	8.8650	0.1182	SLUG	1.4904	7.3734
3031.70	639.02	493.12	565.00	0.2103	0.0000	9.0907	0.1172	SLUG	1.4928	7.2652
3075.01	643.15	493.83	565.00	0.2107	0.0000	9.3289	0.1162	SLUG	1.4953	7.1557
3118.32	647.38	494.55	565.00	0.2109	0.0000	9.5692	0.1152	SLUG	1.4979	7.0451
3161.63	651.72	495.26	565.00	0.2109	0.0000	9.8116	0.1142	SLUG	1.5005	6.9334
3204.94	655.19	495.85	565.00	0.8903	0.0000	7.1072	0.1133	SLUG	3.0127	13.7076
3248.25	658.68	496.44	565.00	0.8814	0.0000	7.1815	0.1125	SLUG	3.0169	13.5308
3291.56	662.20	497.03	565.00	0.8726	0.0000	7.2567	0.1116	SLUG	3.0212	13.3548
3334.87	665.75	497.62	565.00	0.8637	0.0000	7.3332	0.1108	SLUG	3.0255	13.1794
3378.18	669.33	498.22	565.00	0.8550	0.0000	7.4114	0.1099	SLUG	3.0299	13.0048
3421.49	672.94	498.82	565.00	0.8462	0.0000	7.4905	0.1091	SLUG	3.0342	12.8309
3464.80	676.58	499.39	565.00	0.8380	0.0000	7.5670	0.1082	SLUG	3.0384	12.6663
3508.11	680.25	499.99	565.00	0.8293	0.0000	7.6491	0.1074	SLUG	3.0428	12.4937

3551.42	683.96	500.60	565.00	0.8206	0.0000	7.7329	0.1065	SLUG	3.0473	12.3200
3594.73	687.70	501.21	565.00	0.8119	0.0000	7.8188	0.1056	SLUG	3.0518	12.1473
3638.04	691.47	501.82	565.00	0.8032	0.0000	7.9063	0.1047	SLUG	3.0564	11.9745
3681.35	695.28	502.43	565.00	0.7946	0.0000	7.9955	0.1038	SLUG	3.0609	11.8021
3724.66	699.12	503.02	565.00	0.7860	0.0000	8.0868	0.1029	SLUG	3.0656	11.6302
3767.97	703.00	503.64	565.00	0.7778	0.0000	8.1751	0.1020	SLUG	3.0700	11.4671
3811.28	706.91	504.27	565.00	0.7692	0.0000	8.2696	0.1010	SLUG	3.0747	11.2962
3854.59	710.86	504.90	565.00	0.7607	0.0000	8.3660	0.1001	SLUG	3.0794	11.1258
3897.90	714.86	505.53	565.00	0.7522	0.0000	8.4644	0.0991	SLUG	3.0842	10.9558
3941.21	718.89	506.16	565.00	0.7437	0.0000	8.5653	0.0982	SLUG	3.0890	10.7863
3984.52	722.96	506.80	565.00	0.7353	0.0000	8.6678	0.0972	SLUG	3.0938	10.6172
4027.83	727.07	507.41	565.00	0.7268	0.0000	8.7726	0.0963	SLUG	3.0987	10.4485
4071.14	731.23	508.06	565.00	0.7188	0.0000	8.8745	0.0953	SLUG	3.1034	10.2882
4114.45	735.43	508.71	565.00	0.7104	0.0000	8.9838	0.0943	SLUG	3.1084	10.1204
4157.76	739.67	509.36	565.00	0.7020	0.0000	9.0951	0.0933	SLUG	3.1134	9.9530
4201.07	743.96	510.02	565.00	0.6937	0.0000	9.2095	0.0923	SLUG	3.1185	9.7860
4244.38	748.30	510.68	565.00	0.6854	0.0000	9.3266	0.0913	SLUG	3.1236	9.6194
4287.69	752.68	511.35	565.00	0.6771	0.0000	9.4459	0.0903	SLUG	3.1288	9.4531
4331.00	757.11	512.02	565.00	0.6688	0.0000	9.5681	0.0892	SLUG	3.1340	9.2872

** PRESSURE ANALYSIS **

TOTAL FRICTION, LIQUID = 0.0000 PSI
TOTAL POTENTIAL, LIQUID = 0.0000 PSI

TOTAL FRICTION, TWO-PHASE = 15.8859 PSI
TOTAL POTENTIAL, TWO-PHASE = 271.9273 PSI
TOTAL ACCELE., TWO-PHASE = 0.0000 PSI

```
      INTEGER IOPT,IER
              real*8 mdei, arg, y, X
      iopt=2

      THIS PROGRAM IS USED TO DETERMINE THE IDEAL BEHAVIOR
      OF A WELL PRODUCING AT CONSTANT MASS FLOW RATE FROM
      A HOMOGENEOUS RESERVOIR WITH A SEALING FAULT BOUNDARY.
      HERE IS CALCULATED THE EXPONENTIAL-INTEGRAL TO FIND THE
      FLOWING BOTTOMHOLE PRESSURE.


      po= porosity (dimensionless)
      dv= dynamic viscosity (Pa-s)
      tc= total compressesibility (1/Pa)
      co= conductivity (m**3)
      rt= reservoir thickness (m)
      fl= mass flow rate (kg/s)
      sv= specific fluid volume (m**3/kg)
      wr= wellbore radius (m)
      df= distance to the sealing fault (m)
      pe= permeability (m**2)

      phi=3.141592654
      pi=5.695
      p0=.1
      dv=1.0086e-04
      tc=1.865e-09
      co=5.4016e-12
      rt=50.
      fl=16.19
      sv=1.2874e-03
      wr=.108
      df=337.9
      pe=co/rt
      al=fl*sv*dv/(4.e06*phi*pe*rt)
      type *,al
      be=p0*dv*tc/pe
      de=be*wr**2./4.
      el=be*df**2.
      do 20 i=1,10
      ti=10.**i
      arg=de/ti
      y=mdei(iopt,arg,ier)
      type *,y
      arg=el/ti
      x=mdei(iopt,arg,ier)
      type *,x
      pwf=pi-al*(y+x)
      type *,t,pwf,y,x
      write(10,'(4e15.6)') t,pwf,y,x
20    continue
      stop
      end
```

```
      implicit real*8 (a-h),(o-z)
      common/blkcf/v(20),nv
      external pfd

C     THIS PROGRAM CAN BE USED TO DETERMINE THE IDEALIZED BEHAVIOR
C     OF A WELL PRODUCING AT CONSTANT MASS FLOW RATE FROM A
C     HETEROGENEOUS (DOUBLE-POROSITY) RESERVOIR WITH
C     A SEALING FAULT BOUNDARY.
C     HERE IS USED THE STEHFEST ALGORITHM TO FIND THE BOTTOMHOLE PRESSURE



      nv=18

      lambda=4.0973e-08
      omega=.1
      wr=.108
      ra=.108
      df=337.9

      pi=5.695
      fl=16.19
      sv=1.2874e-03
      dv=1.0086e-04
      phi=3.141592654
      co=5.4016e-12

      al=fl*sv*dv*1.e-06/(2.*phi*co)

      call array (v,nv)
      do i=1,nv
      type *,v(i),i
      enddo
      type *,al
      do 1 i=1,10
      do 2 j=1,9
      t=10.**(i-1)*j
      r=ra/wr
      a=pfd(t,r,lambda,omega)
      r=2.*df/wr
      b=pfd(t,r,lambda,omega)
      pfi=pi-al*(a+b)
      Type *,t,pfi,a,b
      write(10,'(4e15.6)') t,pfi,a,b
2     continue
1     continue

      stop
      end
```

```
C
      SUBROUTINE ARRAY(V,N)
C
C     EVALUATES THE ARRAY V(I) FOR N-TERMS IN AN ASYMPTOTIC
C     SERIE EXPANSION OF PROBABILITY DENSITY FUNCTION.
C     FOR SINGLE PRECISION 8-DIGIT ARITHMETIC THE OPTIMUM
C     VALUE FOR N IS ABOUT N=10.  FOR DOUBLE PRECISION
C     ARITHMETIC THE OPTIMUM IS ABOUT N=18.  N MUST BE EVEN.
C     BASED ON 'ALGORITHM 368' BY H. STEINFEST IN COMMUNICAT-
C     IONS OF THE ACM,VOL13,NO.1,JAN 1970.
C
      IMPLICIT REAL*8 (A-H,O-Z)
      DIMENSION G(20),V(20),H(20)
      G(1)=1.
      NH=N/2
      DO 10 I=2,N
 10   G(I)=G(I-1)*I
C
      H(1)=2./G(NH-1)
      DO 20 I=2,NH
      FI=I
      IF (I.EQ.NH) GOTO 15
      H(I)=FI**NH*G(2*I)/(G(NH-I)*G(I)*G(I-1))
      GOTO 20
 15   H(I)=FI**NH*G(2*I)/(G(I)*G(I-1))
 20   CONTINUE
      SN=2*(NH-NH/2*2)-1
C
      DO 30 I=1,N
      V(I)=0.
      K1=(I+1)/2
      K2=I
      IF (K2.GT.NH) K2=NH
      DO 40 K=K1,K2
      IF (2*K-I.EQ.0) GOTO 36
      IF (I.EQ.K) GOTO 37
      V(I)=V(I)+H(K)/(G(I-K)*G(2*K-I))
      GOTO 40
 36   V(I)=V(I)+H(K)/G(I-K)
      GOTO 40
 37   V(I)=V(I)+H(K)/G(2*K-I)
 40   CONTINUE
      V(I)=SN*V(I)
      SN=-SN
C     WRITE (5,90) I,V(I)
 90   FORMAT (3X,I6,3X,G13.6)
 30   CONTINUE
      RETURN
      END
```

```
C
C       LPFD - The Laplace transform of the pressure function for
C              the double porosity model.
C
C       INPUT PARAMETERS -
C         S - The parameter in the Laplace space.
C         R - Radial distance.
C         LAMBDA -
C         OMEGA -
C
C       PROGRAM SUBROUTINES - MMBSK0, MMBSK1. ( The Bessel functions
C              K0 and K1 from the IMSL library.
C
        FUNCTION LPFD(S, R, LAMBDA, OMEGA)

        IMPLICIT REAL*8 (A-H),(O-Z)
        REAL*8 S, R, LAMBDA, OMEGA, LPFD, K0, K1, MMBSK0, MMBSK1
        EXTERNAL MMBSK0, MMBSK1

        FS = (OMEGA*(1. - OMEGA)*S + LAMBDA) / ((1.-OMEGA)*S + LAMBDA)

        X1 = SQRT(S*FS)
        X0 = X1*R

        IOPT = 1
        K0 = MMBSK0(IOPT, X0, IER)
        K1 = MMBSK1(IOPT, X1, IER)

        LPFD = K0/(S*X1*K1)

        RETURN
        END
```

```
C
C     LPINV - Inverse Laplace transformation with the Stehfest algorithm.
C
C     INPUT PARAMETERS -
C       T - Time.
C       R - Radial distance.
C       LAMBDA -
C       OMEGA -
C       LPFD - The laplace transform of the pressure function.
C
C     OUTPUT PARAMETER -
C       PFD - The pressure function.
C
      SUBROUTINE LPINV(T, R, LAMBDA, OMEGA, LPFD, PFD)

      IMPLICIT REAL*8 (A-H),(O-Z)
      REAL*8 T, R, LAMBDA, OMEGA, LPFD, PFD
      EXTERNAL LPFD

      COMMON/BLKCF/V(20), NV

      XLN2 = DLOG(2.D0)
      PP = XLN2/T

      PFD = 0.
      DO I = 1, NV
        S = PP*I
        PFD = PFD + V(I)*LPFD(S, R, LAMBDA, OMEGA)
      END DO

      PFD = PFD*PP

      RETURN
      END
```

```
C
C       PFD - Dimensionless pressure for the double porosity model.
C
C       INPUT PARAMETERS -
C         T  - Time.
C         R - Radial distance.
C         LAMBDA -
C         OMEGA -
C
C       PROGRAM SUBROUTINES - LPINV.
C
        FUNCTION PFD(T, R, LAMBDA, OMEGA)

        IMPLICIT REAL*8 (A-H),(O-Z)
        REAL*8 T, R, LAMBDA, OMEGA, PFD, LPFD
        EXTERNAL LPFD


        CALL LPINV(T, R, LAMBDA, OMEGA, LPFD, PFD)

        RETURN
        END
```

0.100000E+01	0.526693E+01	0.165089E+01	0.000000E+00
0.200000E+01	0.524782E+01	0.195943E+01	0.000000E+00
0.300000E+01	0.523621E+01	0.214686E+01	0.000000E+00
0.400000E+01	0.522783E+01	0.228224E+01	0.000000E+00
0.500000E+01	0.522125E+01	0.238837E+01	0.000000E+00
0.600000E+01	0.521584E+01	0.247571E+01	0.000000E+00
0.700000E+01	0.521124E+01	0.254995E+01	0.000000E+00
0.800000E+01	0.520729E+01	0.261452E+01	0.000000E+00
0.900000E+01	0.520371E+01	0.267165E+01	0.000000E+00
0.100000E+02	0.520053E+01	0.272289E+01	0.000000E+00
0.200000E+02	0.517950E+01	0.306250E+01	0.000000E+00
0.300000E+02	0.516710E+01	0.326263E+01	0.000000E+00
0.400000E+02	0.515828E+01	0.340512E+01	0.000000E+00
0.500000E+02	0.515142E+01	0.351584E+01	0.000000E+00
0.600000E+02	0.514581E+01	0.360641E+01	0.000000E+00
0.700000E+02	0.514106E+01	0.368306E+01	0.000000E+00
0.800000E+02	0.513694E+01	0.374949E+01	0.000000E+00
0.900000E+02	0.513331E+01	0.380812E+01	0.000000E+00
0.100000E+03	0.513006E+01	0.386059E+01	0.000000E+00
0.200000E+03	0.510866E+01	0.420617E+01	0.000000E+00
0.300000E+03	0.509612E+01	0.440854E+01	0.000000E+00
0.400000E+03	0.508722E+01	0.455219E+01	0.000000E+00
0.500000E+03	0.508032E+01	0.466365E+01	0.728676E-37
0.600000E+03	0.507468E+01	0.475473E+01	0.467830E-34
0.700000E+03	0.506991E+01	0.483175E+01	0.713610E-32
0.800000E+03	0.506578E+01	0.489847E+01	0.411554E-30
0.900000E+03	0.506213E+01	0.495733E+01	0.118531E-28
0.100000E+04	0.505887E+01	0.500998E+01	0.203734E-27
0.200000E+04	0.503741E+01	0.535643E+01	0.102349E-20
0.300000E+04	0.502485E+01	0.555912E+01	0.958110E-18
0.400000E+04	0.501595E+01	0.570293E+01	0.531432E-16
0.500000E+04	0.500904E+01	0.581449E+01	0.698057E-15
0.600000E+04	0.500339E+01	0.590564E+01	0.330043E-14
0.700000E+04	0.499862E+01	0.598271E+01	0.311547E-14
0.800000E+04	0.499448E+01	0.604947E+01	-0.345494E-13
0.900000E+04	0.499083E+01	0.610836E+01	-0.195824E-12
0.100000E+05	0.498757E+01	0.616104E+01	-0.575568E-12
0.200000E+05	0.496611E+01	0.650759E+01	0.630288E-10
0.300000E+05	0.495355E+01	0.671032E+01	-0.940759E-09
0.400000E+05	0.494464E+01	0.685416E+01	0.308657E-08
0.500000E+05	0.493773E+01	0.696573E+01	0.672090E-08
0.600000E+05	0.493208E+01	0.705689E+01	-0.831189E-08
0.700000E+05	0.492731E+01	0.713396E+01	-0.542535E-08
0.800000E+05	0.492317E+01	0.720073E+01	0.154805E-06
0.900000E+05	0.491952E+01	0.725962E+01	0.812304E-06
0.100000E+06	0.491626E+01	0.731230E+01	0.268840E-05
0.200000E+06	0.489475E+01	0.765887E+01	0.649719E-03
0.300000E+06	0.488193E+01	0.786160E+01	0.468218E-02
0.400000E+06	0.487250E+01	0.800544E+01	0.133577E-01
0.500000E+06	0.486481E+01	0.811702E+01	0.259258E-01
0.600000E+06	0.485822E+01	0.820818E+01	0.412184E-01
0.700000E+06	0.485239E+01	0.828525E+01	0.582505E-01
0.800000E+06	0.484713E+01	0.835201E+01	0.763053E-01
0.900000E+06	0.484234E+01	0.841091E+01	0.948873E-01
0.100000E+07	0.483791E+01	0.846359E+01	0.113661E+00
0.200000E+07	0.480574E+01	0.881016E+01	0.286395E+00
0.300000E+07	0.478478E+01	0.901289E+01	0.422119E+00
0.400000E+07	0.476916E+01	0.913674E+01	0.530476E+00
0.500000E+07	0.475670E+01	0.926831E+01	0.620083E+00
0.600000E+07	0.474633E+01	0.935747E+01	0.696309E+00
0.700000E+07	0.473745E+01	0.943654E+01	0.762571E+00
0.800000E+07	0.472969E+01	0.950331E+01	0.821143E+00
0.900000E+07	0.472279E+01	0.956220E+01	0.873617E+00
0.100000E+08	0.471658E+01	0.961488E+01	0.921130E+00
0.200000E+08	0.467511E+01	0.996145E+01	0.124411E+01
0.300000E+08	0.465049E+01	0.101642E+02	0.143985E+01
0.400000E+08	0.463473E+01	0.103080E+02	0.157867E+01
0.500000E+08	0.462506E+01	0.104196E+02	0.168782E+01
0.600000E+08	0.461886E+01	0.105108E+02	0.177736E+01
0.700000E+08	0.461439E+01	0.105878E+02	0.185328E+01
0.800000E+08	0.461117E+01	0.106546E+02	0.191918E+01
0.900000E+08	0.460892E+01	0.107135E+02	0.197739E+01
0.100000E+09	0.460242E+01	0.107662E+02	0.202953E+01
0.200000E+09	0.455964E+01	0.111127E+02	0.237367E+01
0.300000E+09	0.453458E+01	0.113155E+02	0.257557E+01
0.400000E+09	0.451678E+01	0.114593E+02	0.271902E+01
0.500000E+09	0.450298E+01	0.115709E+02	0.283035E+01
0.600000E+09	0.449169E+01	0.116620E+02	0.292135E+01
0.700000E+09	0.448215E+01	0.117391E+02	0.299831E+01
0.800000E+09	0.447389E+01	0.118059E+02	0.306498E+01
0.900000E+09	0.446659E+01	0.118648E+02	0.312381E+01
0.100000E+10	0.446007E+01	0.119175E+02	0.317643E+01
0.200000E+10	0.441715E+01	0.122640E+02	0.352276E+01
0.300000E+10	0.439204E+01	0.124668E+02	0.372541E+01
0.400000E+10	0.437423E+01	0.126106E+02	0.386921E+01
0.500000E+10	0.436041E+01	0.127222E+02	0.398076E+01
0.600000E+10	0.434911E+01	0.128133E+02	0.407191E+01
0.700000E+10	0.433957E+01	0.128904E+02	0.414897E+01
0.800000E+10	0.433130E+01	0.129572E+02	0.421573E+01
0.900000E+10	0.432400E+01	0.130161E+02	0.427461E+01